



# UNIVERSITAT DE BARCELONA

Final Degree Project  
**Biomedical Engineering Degree**

**“Computational model of the fetal heart  
with Coarctation of the Aorta “**

Barcelona, 8 de Juny de 2022

Author: Adriana Costafreda

Director/s: Patricia Garcia Cañadilla & Bart Bijmens

Tutor: Fátima Crispi

## Abstract

It is thought that altered intrauterine hemodynamics may lead to congenital heart defects, such as aortic arch abnormalities. Coarctation of the aorta (CoA) is one of the most difficult cardiac defects to diagnose before birth, because of the patency of the ductus arteriosus (DA). It consists of a narrowing in the aortic isthmus (AoI) causing a decrease of blood flow. Prenatal diagnosis is important to reduce mortality and morbidity. Nonetheless, prenatal diagnosis has a high rate of false-positive and false-negatives and local hemodynamics in the CoA is not fully understood. The aim of this project was to improve our understanding of the underlying cause of CoA using computational fluid dynamics (CFD) tools. We have implemented a computational model with an idealized geometry of the fetal aorta to investigate the relationship between flow unbalance and wall shear stress (WSS) at the isthmus-ductus. An imbalanced flow was imposed in the ascending aorta (AscAo) and ductus to study if a progressive aortic flow reduction suggests the “flow-dependency” of the fetal aortic arch development. As a result, when aortic flow diminished from 50% to 10% progressively, velocity and WSS decreased in the aortic arch and increased in the distal arch. A redistribution of flow could be observed in the model and a “zero flow zone” could be noticed between the brachiocephalic artery and left carotid when the flow decreased to from 50% to 10%. Additionally, another “zero flow zone” could be observed in the AoI when the aortic flow decreased from 50% to 30%.

**Keywords:** Computational model, Coarctation of the aorta, Computational Fluid Dynamics, wall shear stress, flow imbalance, flow-dependency

## Tabla de contenido

ACKNOWLEDGEMENTS .....	5
LIST OF FIGURES.....	6
LIST OF TABLES .....	7
GLOSSARY OF TERMS .....	8
1. GENERAL INTRODUCTION .....	9
1.1. Motivation and Research Objectives .....	10
1.2. Methodology .....	11
1.3. Structure of the project .....	11
1.4. Scope and limitations.....	12
1.5. Location of the Project.....	13
2. BACKGROUND .....	14
2.1. State of the art .....	14
2.1.1. Coarctation of the Aorta .....	14
2.1.2. Computational models of the fetal coarctation of the aorta .....	17
2.2. State of the Situation .....	19
2.3. Hypothesis .....	20
3. MARKET ANALYSIS.....	21
3.1. Market drivers .....	21
3.2. Evolution of the market .....	21
3.3. Future perspectives of the market .....	23
4. EXECUTION CHRONOGRAM .....	24
4.1. Work Breakdown Structure (WBS) .....	24
4.2. Execution Chronogram of the global project (GANTT) .....	24
5. CONCEPTION ENGINEERING .....	27
5.1. 0D lumped model of the fetal aortic arch .....	27
a) Input data.....	27
b) Design of the 0D model .....	27
5.2. CFD modelling of the fetal aortic arch .....	28
a) Design of the 3D geometry .....	28
b) Solid Modeling .....	28
c) Building the 3D surface mesh .....	29
d) CFD simulations with Sim Vascular .....	29
e) Post Processing.....	29

5.3.	Parametric study: hemodynamical assessment of CoA with different degrees of diminished flow in the aortic arch.....	30
6.	DETAIL ENGINEERING .....	31
6.1.	0D lumped model of the fetal aortic arch .....	31
a)	Input data .....	31
b)	Design of the 0D model .....	32
6.2.	CFD modelling of the fetal aortic arch .....	32
a)	Design of the 3D geometry .....	32
b)	Solid Modeling .....	35
c)	Building the 3D surface mesh.....	35
d)	CFD simulations with Sim Vascular .....	36
e)	Post Processing.....	39
6.3.	Parametric study: hemodynamical assessment of CoA with different degrees of diminished flow in the aortic arch.....	40
6.4.	Results.....	45
6.5.	Discussion .....	48
7.	TECHNICAL FEASIBILITY: SWOT Analysis .....	49
8.	ECONOMICAL FEASIBILITY.....	51
9.	REGULATION AND LEGAL ASPECTS.....	53
10.	CONCLUSIONS AND FUTURE RESEARCH.....	54
11.	REFERENCES.....	55
12.	ANNEX.....	59
12.1.	MatLab code .....	59
12.2.	CFD simulations with Sim Vascular .....	62

## ACKNOWLEDGEMENTS

I would like to express my sincere gratitude to my supervisors Patricia Garcia-Cañadilla and Bart Bijmens for giving me the opportunity to work in this project with no prior knowledge on computational models. Thank you for helping and guiding me during the whole project and giving me the resources to successfully carry out my project. Also, I would like to thank them both for giving me the opportunity to assist two important workshops which were key to learn how to build computational fluid dynamics models. Finally, I would like to express my gratitude to my friends and to my family for their unconditional support.

*This research was supported by Fundació La Marató de TV3 – Ref 202016-30-31*

## LIST OF FIGURES

<b>Figure 1.</b> Aortic arch anatomy in neonates. Extracted from [3] .....	9
<b>Figure 2.</b> Coarctation of the aorta. Left, preductal coarctation is narrowing of the DescAo before the ductus arteriosus. Right, postductal coarctation is narrowing of the DescAo after the ductus arteriosus. Extracted from [11].....	14
<b>Figure 3.</b> Fetal circulation. Extracted from [13].....	15
<b>Figure 4.</b> The two main theories for the pathogenesis of aortic coarctation. A) Skodaic hypothesis. B) Hemodynamic hypothesis. Extracted from: [8] .....	16
<b>Figure 5.</b> EDT diagram .....	24
<b>Figure 6.</b> GANTT diagram of the global project.....	26
<b>Figure 7.</b> The Sim Vascular pipeline leads the user from solid modeling of the imported geometry to completion of blood flow simulations.....	28
<b>Figure 8.</b> Schematic diagram of the 3D aortic arch model. Extracted from [31] .....	32
<b>Figure 9.</b> Sketch in FREECAD <sup>3</sup> for the aortic arch.....	34
<b>Figure 10.</b> Left, Sketch in FREECAD <sup>3</sup> of the outlines of the neck vessels, AscAo, DescAo, and DA. Right, Final 3D geometry of the fetal arch and ductus designed using FREECAD <sup>3</sup> .....	34
<b>Figure 11.</b> 3D Mesh of the ArchAo and DA.....	36
<b>Figure 12.</b> Inlet boundary condition for the first seven time steps in the ductus .....	37
<b>Figure 13.</b> Circuit representation of RCR block. Extracted from [33] .....	37
<b>Figure 14.</b> CFD model for the fetal ArchAo and DA. ....	38
<b>Figure 15.</b> Inlet and Outlet boundary conditions in Sim Vascular. ....	39
<b>Figure 16.</b> Inflow profile for baseline conditions.....	40
<b>Figure 17.</b> Representation of the different degrees of diminished flow in the ArchAo and increased flow in the DA simulated.....	41
<b>Figure 18.</b> Left, 50% aortic flow and 50% ductal flow. Right, 40% aortic flow and 60% ductal flow. ....	42
<b>Figure 19.</b> Left, 30% aortic Flow and 70% ductal flow. Right, 20% aortic flow and 80% ductal flow. ....	43
<b>Figure 20.</b> 10% aortic flow and 90% ductal flow. ....	43
<b>Figure 21.</b> Different degrees of diminished flow in the left ventricle. ....	44
<b>Figure 22.</b> Different degrees of increased ductal flow. ....	44
<b>Figure 23.</b> Velocity streamlines and WSS in baseline conditions for aortic and ductal flow.....	45
<b>Figure 24.</b> Velocity streamlines and WSS with a 50% aortic flow and 50% ductal flow.....	45
<b>Figure 25.</b> Velocity streamlines and WSS with a 40% aortic flow and 60% ductal flow.....	46
<b>Figure 26.</b> Velocity streamlines and WSS with a 30% aortic flow and 70% ductal flow.....	46
<b>Figure 27.</b> Velocity streamlines and WSS with a 20% aortic flow and 80% ductal flow.....	46
<b>Figure 28.</b> Velocity streamlines and WSS with a 10% aortic flow and 90% ductal flow.....	47
<b>Figure 29.</b> SV Modeling module in Sim Vascular with the imported solid model. ....	62
<b>Figure 30.</b> SV Meshing module in Sim Vascular with the generated 3D mesh.....	62

## LIST OF TABLES

<b>Table 1.</b> Tasks involved in this TFG .....	24
<b>Table 2.</b> Data to simulate the 0D lumped model in Simulink .....	31
<b>Table 3.</b> Artery geometric measures of a fetus .....	33
<b>Table 4.</b> Equations describing the diameter of the different arterial segments of the different of the ArchAo circulation lumped model. Extracted from [19] .....	33
<b>Table 5.</b> Mesh statistics .....	35
<b>Table 6.</b> RCR lumped parameters .....	38
<b>Table 7.</b> Computed factors to model a diminished flow in the AscAo accompanied by an increased flow in the DA.....	42
<b>Table 8.</b> SWOT analysis of the global project.....	49
<b>Table 9.</b> Economical cost of the learning process which needed to be done to carry out the global project.....	51
<b>Table 10.</b> Human resources budget.....	52

## GLOSSARY OF TERMS

**CoA** – Coarctation of the aorta

**CHD** – Congenital Heart Disease

**LSA** - Left Subclavian Artery

**DA** – Ductus arteriosous

**AoI** – Aortic Isthmus

**ArchAo** – Aortic Arch

**CFD** – Computational Fluid Dynamics

**3D** – Three dimensional

**WSS** – Wall Shear Stress

**0D** – Zero dimensional

**CO** – Cardiac Output

**AscAo** – Ascending Aorta

**DescAo** – Descending Aorta

**VSD** – Ventricular Sept Defect

**1D** – One-dimensional

**4D** – Four dimensional

**BCA** – Brachiocephalic artery

**LCCA** – Left Common Carotid Artery

**GA** - Gestational age

**EFW** - Estimated fetal weight

**2D** – Two dimensions

**PAA** – Proximal Aortic Arch

**DAA** – Distal Aortic Arch



## 1. GENERAL INTRODUCTION

Coarctation of the aorta (CoA) is one of the most common congenital heart defects (CHD), accounting for approximately 7% of all live births with CHD. CoA is characterized by an abnormal narrowing of the aorta. In more than 90% of cases, this narrowing is located between the origin of the left subclavian artery (LSA) and the ductus arteriosus (DA), also known as the aortic isthmus (AoI) (Figure 1). The severity of the coarctation can range from a slight narrowing of the distal end of the arch to severe hypoplasia of the entire arch. [1] This obstruction may reduce the blood flow in the fetal aortic arch (ArchAo), leading to arch hypoplasia, although in some cases this may be clinically evident after birth, or even in later life. [2]

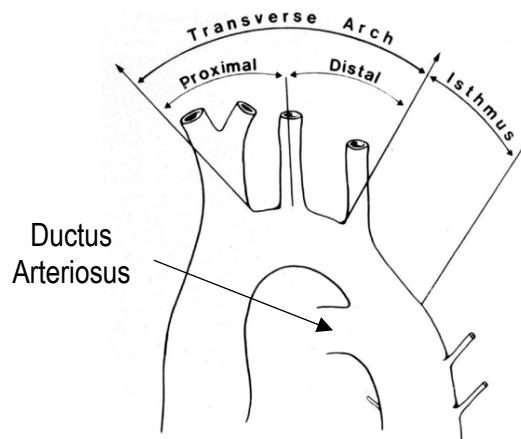


**Figure 1.** Aortic arch anatomy in neonates. Extracted from [3]

CoA is a congenital lesion that occurs in 2.5 to four per 10 000 live births and accounts for the 5%-10% of all CHD. It can be simple (isolated defect) or complex (associated with other cardiac defects) and is classified into two main groups: critical coarctation of the aorta and asymptomatic coarctation. Critical coarctation, accounts for the 60% of all coarctations, and causes symptoms within two months of birth and if is untreated causes death, whereas asymptomatic coarctation presents later, with hypertension in the upper limbs. [4]

In neonates, CoA is a common cause of shock and death since it is often undiagnosed. Despite advances in fetal echocardiography and the description of antenatal findings associated with CoA, this defect remains the most challenging cardiac diagnosis to be made in fetal and early neonatal life due to the patency of the DA. [5] The prenatal detection rate of this condition is disappointingly low, being CoA, the most life-threatening cardiovascular condition overlooked in the early neonatal period, with affected neonates often leaving the hospital undiagnosed and returning in a critical condition. [6]

Prenatal diagnosis is of critical importance to improve survival and reduce morbidity. In most severe cases, suspicion rises when there is ventricular disproportion, however; current echography methods lead to both, high rate false-positive and false-negative rate during diagnosis. Additionally, the hemodynamic remodeling induced by the disease is yet not fully understood, partly due to the wide variety of fetal aortic coarctation types and degrees of severity. [7]

Accordingly, there is a need to develop new technologies that allow accurate prenatal diagnosis of aortic coarctation and that help clinicians to better understand the disease. [7] For this reason, researchers are focusing on improving CoA diagnosis and understanding. Computational fluid dynamics (CFD) is an important tool in this context since it can provide hemodynamic parameters, which can be then interpreted by the doctors and help in the diagnosis and gain a better understanding of the malformation.

Thereby, our purpose is to perform CFD simulations based on a three-dimensional (3D) model of the fetal ArchAo and ductus using Sim Vascular to improve the understanding on the cause of CoA by investigating the relationship of flow unbalance and wall shear stress (WSS) at the isthmus-ductus.

### 1.1. Motivation and Research Objectives

Fetal hemodynamic changes in CoA are not yet fully understood, and current imaging methods are limited to accurately diagnose this congenital effect. Despite various theories have been proposed, the exact pathophysiological mechanisms that lead to the development of CoA are still poorly understood. It is thought that the etiology and pathophysiology of CoA are, to some extent, mostly related to two proposed hypotheses. The hemodynamics hypothesis which suggests a reduced flow across the aortic isthmus and increased flow in the ductus and the skodaic hypothesis which refers to the migration and contraction of the ductal tissue and closure of the patent DA postnatally. [8]

This final degree project aims to develop a computational model which can be used to improve our understanding on the underlying cause of CoA. The author aims to prove the proposed hemodynamic hypothesis by developing a CFD model. An unbalanced flow is imposed to mimic the effects of a diminished flow in the fetal ArchAo to suggest the “flow-dependency” of the fetal aortic arch development, since the hypothesis puts forward the presence of a diminished flow in the pathogenesis of CoA. The CFD model will simulate local hemodynamics such as WSS and velocity streamlines in the fetal aortic arch.

The main objective of this work is to implement a computation model with an idealized geometry of the fetal aorta to investigate the relationship between flow imbalance and WSS at the isthmus-ductus. This will be done hypothesizing that there is a definable relationship between ArchAo geometry and underlying vascular flow.

**Specific aim 1:** To build a simplified CFD model based on an idealized 3D geometry of the fetal aortic and ductal arches to simulate pulsatile hemodynamics including velocity, pressure and WSS.

**Specific aim 2:** To investigate the effects of diminished flow in the fetal aorta by means of CFD simulations with different proportion of flows between the aortic and ductal arch to improve our understanding of the cause of CoA.

## 1.2. Methodology

A computational model of the ArchAo and DA was built based on an ideal geometry designed using a free available software. Pulsatile hemodynamics were simulated as aortic flow decreased from its baseline conditions to 50%, 40%, 30%, 20% and 10%, with accompanying ductal flow increased proportionally by 50%, 60%, 70%, 80% and 90%. In order to mimic the blood flow behaviour in the fetal aortic arch and ductus, a zero-dimensional (0D) lumped model was used to obtain the outlet boundary conditions. The lumped model was used to obtain the parameters for the Windkessels in the outlets of the model, imposing a 30% of flow going to the upper part of the body and a 70% of flow to the lower body. A CFD software was used to carry out the flow simulations and a visualization software was used to evaluate and visualize the important hemodynamic parameters obtained from the simulation results.

## 1.3. Structure of the project

Firstly, to carry out successfully the final degree project, it was essential to understand the basis of coarctation of the aorta and what hemodynamic parameters needed to be used to understand the malformation. To do so, literature research on what computational models had been developed to simulate blood-flow in fetuses with coarctation of the aorta was an important step of the project.

In the second phase of the project, a 0D model of the fetal aortic arch and ductus was used to determine the outlet boundary conditions for the model. The 0D model was provided by previous work and it was used to obtain the proximal resistance, distal resistance, and capacitance of the four Windkessels which were imposed in the outlets of the model.

The third phase consisted in generating the 3D model and performing the CFD simulations. To do so, a 3D geometry needed to be designed. To design the geometry a 3D modeler software was used. Tutorials were useful for the author to learn how to design the 3D geometry using the software. Hereinafter, to do the CFD simulations an open-source CFD software was used. Tutorials and documentation were useful as well for the author to learn how to import the 3D model, generate the mesh and do the flow simulations. Moreover, exhaustive research on the topic needed to be done to learn how to correctly run the simulations the author required.

In the fourth phase, the final simulations were carried out. Based on the final geometry of the aortic arch, a hemodynamics simulation in the two arches is performed using CFD. Pulsatile hemodynamics, including velocity, pressure gradient, and WSS were simulated imposing an unbalanced flow between the two inlets of the model. A parametric analysis was carried out to investigate the relationship between flow unbalance and WSS at the isthmus-ductus zone. The author simulated as aortic flow decreased from its baseline conditions to 50%, 40%, 30%, 20% and 10%, with an accompanying ductal flow increased proportionally to maintain combined cardiac output (CO). Furthermore, the author also verified that the flow distribution was correct along the ArchAo and ductus and a 30% of flow was going to the upper body and 70% to the lower body.

The fifth phase started once the model was validated. When the simulations were correctly done and the parametric analysis was carried out, results could be obtained. A post processing of the final simulation results was performed by the author. A visualization software was used to study the WSS in the aortic-isthmus zone and the streamlines in the model. A clear interpretation of the hemodynamic parameters is done, and the results are well discussed to present the final conclusions of the work.

#### 1.4. Scope and limitations

The scope of the project is to build a CFD model based on an ideal geometry of the fetal aortic and ductal arch to investigate the relationship between flow imbalance and WSS at the aortic isthmus. This flow imbalance in the two inlets of the model has been simulated by means of CFD to evaluate whether there is an increased wall shear stress in the site where the coarctation usually takes place.

To do the simulations, a laminar blood flow is set in the inlets of the model, ascending aorta (AscAo), and ductus, whereas in the outlets of the model, a RCR Windkessel condition is imposed. The proposed model was able to mimic realistic blood flow distribution in the fetal aortic arch, ensuring that, in healthy conditions, 30 % of the total CO goes to the upper body and the 70 % of the blood flow travels through the descending aorta (DescAo) to the lower body parts.

The TFG includes:

- The use of a 0D model of the fetal ArchAo to find the values for the components of the windkessels in outlets of the model.
- The design of a 3D geometry of the fetus ArchAo and ductus.
- Building a 3D mesh in Sim Vascular.
- Running the CFD simulations in Sim Vascular.
- A parametric study of the different flow proportions (50-50, 60-40, 70-30, 80-20, 90-10) to investigate the relationship between dismissed blood flow in the ArchAo and wall shear stress.
- Parametric analysis changing the parameters of the RCR Windkessel's to make the CFD simulations as realistic as possible.
- Post-processing of the 3D simulation results using Paraview to analyze the WSS in the ArchAo geometry and visualize the velocity profiles to confirm the initial hypothesis.

The scope of this project is in accordance with the accomplishments of its objectives, but also there are several limitations because it is a final degree project and therefore has important time and economical constraints.

The TFG excludes:

- Decreasing the aortic isthmus diameter to mimic the coarctation of the aorta.
- The use of a real control geometry and a real geometry with CoA. The geometry we designed is ideal since it was not possible to use CT scans to segment the model.
- The simulation is only performed for one cardiac cycle which does not correctly simulate the whole behavior of the systemic blood circulation in the fetus. This
- The walls of the ArchAo and arteries are considered to be rigid and not elastic, excluding the elastic properties of the vessels. This has been done to reduce the complexity of the blood flow simulations.

Moreover, an important limitation of the project is the complexity of aortic flow patterns, since it is challenging to accurately select the appropriate boundary conditions, replicating vascular compliance.

### 1.5. Location of the Project

The project was proposed by the group of Translational Computing in Cardiology in IDIBAPS (Institut d'Investigacions Biomèdiques August Pi I Sunyer). IDIBAPS is a biomedical research institute which combines clinical and basic research to accelerate the translation of the knowledge to the benefit of the patients. [9]

The group of Translational computing in cardiology lead by Bart Bijnens aims at developing and investigating computing for understanding each individual heart, to improve diagnosis, prognosis, and therapy. They work interdisciplinary combining biomedical engineering, physics, and mathematics with basic research, as well as clinical expertise, to link technological and theoretical science with physiological and clinical knowledge. [10] The group proposed an approach to gain a better understanding of the congenital defect using CFD models. A model can be build based on the geometry of the ArchAo of a fetus and CFD simulations can be carried out to investigate the relationship between flow unbalance and wall shear stress at the isthmus-ductus.

## 2. BACKGROUND

### 2.1. State of the art

To have a better understanding of the field that this project covers, some concepts are defined and the state-of-art behind these concepts is presented.

#### 2.1.1. Coarctation of the Aorta

CoA is a congenital heart defect, describing an abnormal narrowing of the aorta which has developed in the embryo and is present from birth. Anatomically a coarctation of the aorta is a shelf of tissue extending from the postero-lateral aortic wall towards the ductus arteriosus. [4] There are different types and degrees of CoA depending on the location and the extent of the narrowing (Figure 2). The most common type of CoA is the preductal coarctation (Figure 2 *left*), which is located affecting the aortic isthmus, with or without hypoplasia of the transverse arch. The postductal case, is more rarely found, and it affects the lower thoracic or abdominal aorta (Figure 2 *right*). [4]

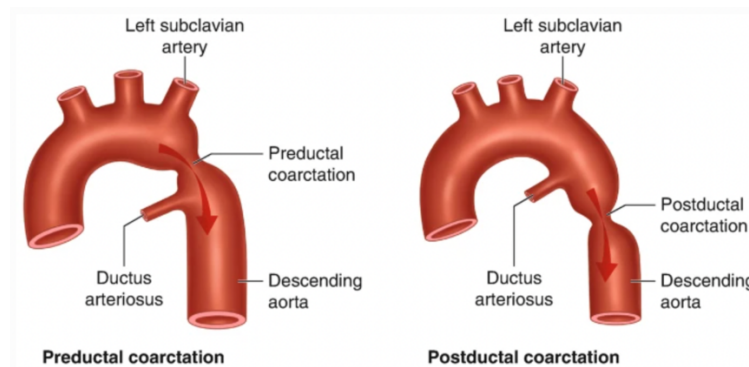


**Figure 2.** Coarctation of the aorta. Left, preductal coarctation is narrowing of the DescAo before the ductus arteriosus. Right, postductal coarctation is narrowing of the DescAo after the ductus arteriosus. Extracted from [11]

Coarctation is often associated with other defects. Bicuspid aortic valve and ventricular septal defect (VSD) represent the two most common associated defects, present in 40% to 50% and 25% to 40%, respectively. CoA is also frequently associated with complex heart disease and other left-sided obstructive lesions. [12]

Prenatal diagnosis of coarctation can be extremely difficult because of the presence of the ductus and the parallel circulation that exists before birth. [1] In a fetus, blood circulation is different as in adults because the placenta is doing the work that the baby's lungs will do after birth. In fetal life (see Figure 3), there are three shunts which connect the systemic circulation with the pulmonary circulation, therefore, the cardiovascular system operates in parallel. One of the shunts is the ductus arteriosus which connects the main pulmonary artery with the aorta, thus allowing blood to bypass from the pulmonary artery to the systemic circulation. [13]

On the grounds that there is this parallel circulation in fetal life, fetuses with CoA are asymptomatic because they can compensate the narrowing of the ArchAo by redistributing the blood through the ductus arteriosus. However, when the baby is born, the separation from the placental circulation results in increased systemic vascular resistance, while initiation of ventilation lowers pulmonary vascular resistance. These combined factors, with the associated increased oxygenation, result in closures of the three shunts, including the foramen ovale, ductus arteriosus, and ductus venosus and the parallel circulation becomes a serial circulation. [14] In postnatal life, the closing of the ductus is determinantal in babies with CoA since the coarctation blocks normal blood flow to the body. Clinical outcome varies from mild systemic hypertension to serious heart failure and death. The clinical manifestations are variable and depend on the severity of the malformation. A rapid progression with heart failure can be seen in the neonate, but sometimes children are lately diagnosed, after a high blood pressure is detected. [2]

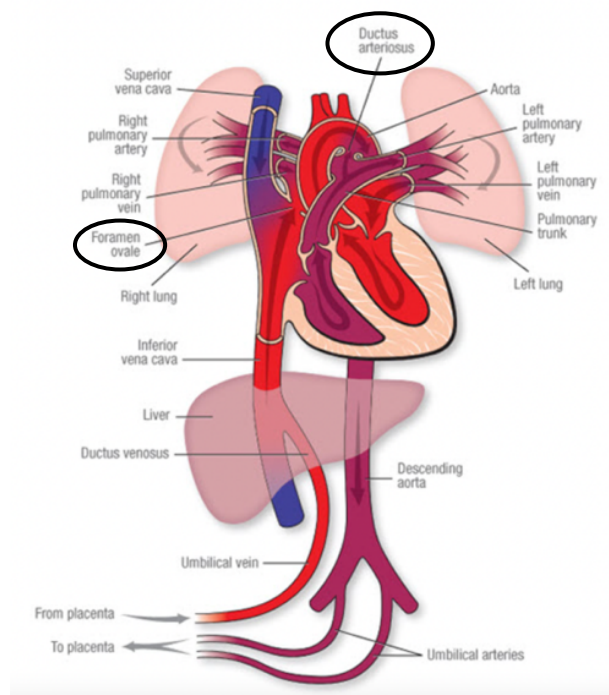


**Figure 3.** Fetal circulation. Extracted from [13]

CoA develops early in fetal life, in the first weeks of pregnancy, when the development of all major arteries takes place. Despite various theories that have been proposed, the exact pathophysiological mechanisms that lead to the development of CoA are still poorly understood. One of the morphological abnormalities proposed as an explanation for CoA concerns fetal blood flow. The **hemodynamic theory** postulates that reduced or reversed flow at the isthmus leads to the distal arch becoming a functional branch of the DA. This hypothesis is related to the hypoplasia of the left heart which is associated with decreased anterograde flow through the developing left ventricle in the fetus. It is thought that the pattern of flow in the fetal circulation influences embryogenesis; in particular, a reduction in the volume of blood passing through the AAO during the fetal period in CoA. [8] This diminished aortic flow leads postnatally to the development of CoA. [15] The flow theory is supported by the fact that intracardiac anomalies with decreased aortic flow patterns have an increased incidence of CoA and other arch anomalies.

The second speculation in the origin of CoA is referred as Skodiatic hypothesis. It suggests that the ductus smooth muscle tissue migrates into the periductal aorta and subsequently causes constriction after birth. [12]

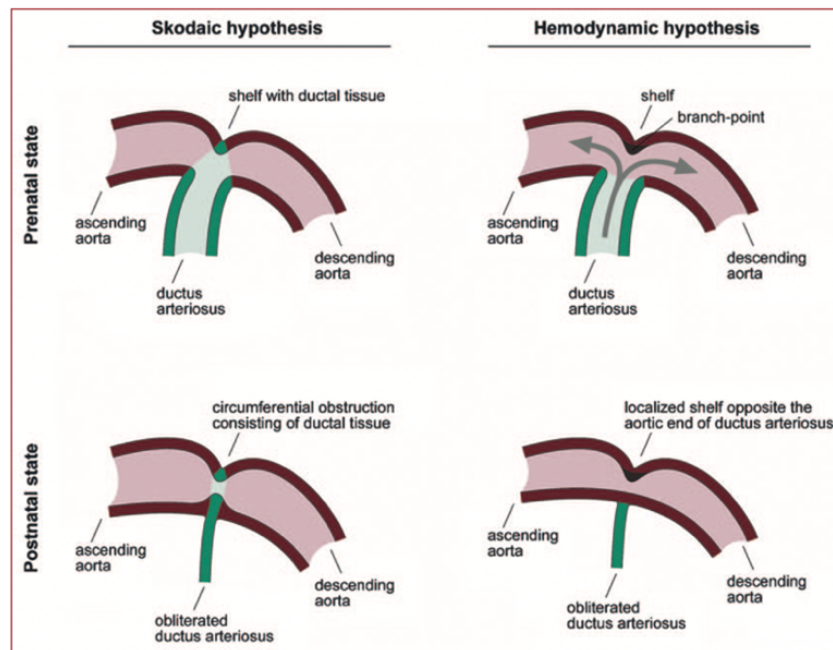


**Figure 4.** The two main theories for the pathogenesis of aortic coarctation. A) Skodiatic hypothesis. B) Hemodynamic hypothesis. Extracted from: [8]

When fetal diagnosis of coarctation is made or suspected, the treatment is the use of intravenous Prostaglandines type1 to avoid the closure of the ductus arteriosus immediately after birth and to gain time before surgery. For the surgical repair of coarctation several techniques are available. Transcatheter treatment is also an accepted alternative for surgery with comparable results. Despite good results for surgical and transcatheter treatment, long-term morbidity and mortality remains substantial. Early management by correct diagnosis, preferably during fetal life, can reduce long-term complications. [2]

Diagnosis of CoA is mainly based, non-invasively, by fetal echocardiography. Doppler echocardiography can be used to evaluate the severity of CoA. Currently, in clinical practice ultrasonographic evaluation, including measurement of right and left ventricular size, isthmus, and ductal diameters, are used to diagnose aortic coarctation. [7] This is because, suspicion for coarctation of the aorta is usually raised when there is ventricular disproportion in fetal life. Still, the measurements have low sensitivity and specificity. [2] Only 35% of the cases with CoA are detected in the prenatal stage [16], and only in 30-40% of the cases the diagnosis was confirmed postnatally. [6] This leads to both high false-negative and false-positive rates. The reason is that the diagnosis relies on indirect, non-specific signs such as ventricular disproportion, discrepancy of the great vessels (with a pulmonary artery diameter bigger than the aorta) and the evaluation of the aortic arch (anatomic measurements and Doppler flow). [17] [2] [18]



Additionally, the induced hemodynamic and structural remodeling of CoA is not fully understood and the ability to discriminate between true-positive and false-positive cases remains a challenge. [7] [19] Therefore, there is a need to develop new technologies which can help understanding the hemodynamics of the malformation and improve prenatal diagnosis.

Lumped and CFD models have been suggested as a good approach to simulate and model the hemodynamics in human aorta. These can be used to assess and understand hemodynamic changes in the circulation in a non-invasive manner and can be used to study the cause, improve diagnosis and prognosis for CoA.

### **2.1.2. Computational models of the fetal coarctation of the aorta**

In computational models, the computational complexity has increased from 0D models (lump-model) to one-dimensional (1D) and 3D models. The applications of these extend from estimating certain hemodynamic parameters to simulating local flow field. Nowadays, most innovative techniques include a combination of models with different dimensions. [20]

The selection of the model depends on its application scenario and a balance between computational complexity and physiological accuracy that is needed in the investigation. The 0D and 1D models are acceptable for estimating blood flow distribution in the fetal ArchAo and DA. However, to identify important hemodynamic factors, such as WSS and velocity streamlines, 3D models are required. [20]

CFD is a well-established technique in modeling heat, mass, and momentum transfer, which is especially applicable in many areas of engineering, including biomedical among others. Specially, CFD simulations play a significant role in the development and testing of products, as it allows engineers to understand fluid interaction without the need of physically building and testing. [21]

Although CFD can be applied in many areas of research, applications of CFD techniques in cardiology to aid diagnosis and treatment of cardiovascular disease have entered the research domain in recent years. When in vitro and in vivo experiments are not feasible, CFD becomes one of the new methodologies for such investigations. Although CFD alone cannot provide answers to all cardiovascular diseases fully, the results of the numerical simulation can often help to better understand the mechanism and to design in vitro and in vivo experiments to ask questions and provide answers to them. [21]

CFD applications obviate the need for risky invasive measurement techniques but also provide measurements of particular hemodynamic parameters that cannot otherwise be measured directly, such as WSS. CFD can be conveniently used to investigate factors that impact on hemodynamics and pathophysiology of cardiovascular diseases. [21]

To study the effect of CoA, several CFD models have been developed. Many of them, aim to study the effect of CoA after birth, but very few research has been done regarding the origin of CoA prenatally. This work proposes an innovative approach to explain the origin of CoA to improve our understanding. Models in 0D have been developed for the fetal aortic arch and ductus to enable researchers to study flow distributions in fetal life. Patient-specific lumped models of the fetal circulation have shown to be a great approach to understanding mechanisms of fetal hemodynamics, both under healthy and pathological conditions. [19] [22] [7] Nevertheless, to gain a better understanding on the effect of wall shear stress in the ArchAo, 3D models need to be developed.

Lumped models are based on the analogy between fluid dynamics and electric circuits. Blood pressure is analogue to voltage, blood flow to current, and blood flow properties such as viscosity, inertia and compliance are represented by resistors, inductors, and capacitors. In 2014, Garcia-Canadilla et al implemented the first patient-specific model modeling the whole fetal circulation to quantify blood flow redistribution in fetuses with intrauterine growth restriction and to estimate vascular properties that cannot be directly assessed from clinical measurements. [19] In 2017, Paula Giménez Mínguez et al, proposed the use of a lumped model of the fetal circulation to provide insights into the hemodynamic changes in fetuses with aortic coarctation, and this helping to improve its diagnosis. To do so, a patient-specific lumped model of the fetal circulation was implemented which included the modeling of different types and degree of aortic coarctation. The results of this study showed obvious changes in the fetal hemodynamics when there was an 80% of coarctation which corresponded to the clinically used cut-off for pressure drop of 20 mmHg. Furthermore, it was also observed that hemodynamic changes were different depending on the location and degree of the coarctation. [7] Later, in 2017 Àngels Calvet Mirabent carried out his bachelor's thesis with the purpose to understand and predict the hemodynamic modelling in babies with CoA by means of clinical imaging and computational modelling. To do so, the author used echocardiographic data from a cohort of 129 patients with a prenatal diagnosis of suspicion of aortic coarctation and to describe the hemodynamic changes from fetal to neonatal circulation. Then, the author implemented a lumped model of the fetal and neonatal circulation to perform different parametric studies. As a result, the author observed how blood flow velocities in the ArchAo from control fetuses and fetuses with CoA were indistinguishable from each other. [23]

Nonetheless, 0D models have a main limitation, because are only capable of studying flow distribution patterns and pressure gradients in a patient-specific model. To study other relevant hemodynamic parameters such as WSS, 3D models need to be used and CFD simulations need to be carried out to simulate the flow distribution in the model.

In 2017, Zhuo Chen MD et al developed a hemodynamic model of aortic and ductal arches using CFD and 3D/four-dimensional (4D) spatio-temporal image correlation (STIC) fetal echocardiography to investigate the hemodynamics of CoA in human fetuses. The study revealed how progressive narrowing in the aortic isthmus resulted in alterations in flow profile, velocity, pressure, and WSS in the aortic isthmus in normal and CoA model. It could be seen that a 55% reduction in the dimension of aortic isthmus was associated with exponential change in velocity, pressure, and WSS, a probable threshold for hemodynamically significant CoA. [24]

Nonetheless, the approach proposed by Zhuo Chen MD et al does not consider the diminished flow in the aortic arch to explain the cause of CoA. This is what the author puts forward in this project, the evaluation of how a diminished flow in the ArchAo and an increased flow in the ductus influences an increase in WSS in the aortic isthmus, resulting in a change of shape.

However, a study carried out by Zhuo Chen et al in 2020 proposes a similar approach to investigate the effects of diminished flow in the fetal aorta. The study showed that as aortic flow diminished from 100% to 20% progressively, velocity, pressure, and WSS decreased in systole and diastole in the ArchAo and isthmus. These results suggest the “flow-dependency” of the fetal aortic arch development and a unifying hypothesis of diminished flow in the pathogenesis of CoA. [25]

## 2.2. State of the Situation

This project is part of a big project which was funded by La Marató in 2020. Previous work has been done in relation to CoA. 0D lumped models have been developed by the group to investigate the flow distribution and pressure gradients in CoA. However, to evaluate how WSS affects the geometry it is necessary to build 3D models capable of evaluating the effect of wall shear stress in the aortic isthmus.

A project in the group was carried out to understand and predict the hemodynamic remodeling in babies with CoA by means of imaging and computer modelling. Echocardiography data of patients with CoA was analyzed and compared to control data to describe the hemodynamic changes from fetal to neonatal life. A lumped model of fetal circulation was implemented to further understand the hemodynamic changes. A parametric study was carried out to evaluate the effects of ventricular disproportion with different degrees of CoA. The study was able to prove that the blood flow velocities in the ArchAo from control fetuses and fetuses with CoA were distinguishable. [23]

Additionally, the group worked on proposing the use of a lumped model of the fetal circulation to provide insights into the hemodynamic changes in fetuses with aortic coarctation, and thus helping to improve its diagnosis. A patient-specific lumped model of the fetal circulation was implemented in OpenCOR, and different degrees of aortic coarctation were modeled. A parametric study of degree and type of coarctation was performed, where blood flow distribution, cerebroplacental ratio, pressure drop over the coarctation and left ventricular pressure were quantified. The results showed obvious changes in the fetal hemodynamics for 80% of coarctation, which corresponded to the clinically used cutoff pressure drop of 20 mmHg. Furthermore, it was observed that hemodynamic changes were different depending on the location and degree of the coarctation. [7]

The project aims to obtain a more complex model, capable of studying the local field hemodynamic changes such as WSS in CoA. A 3D model will be used to evaluate if there is an increase in WSS because of a diminished flow in the ArchAo. This will be developed to improve our understanding on the hemodynamics of CoA, so clinicians have more information to diagnose and improve the prognosis of fetuses with CoA.

### 2.3. Hypothesis

The report aims to obtain a validation that it is feasible to create a hemodynamic model of the human fetal aortic arch using a 3D geometry and CFD.

The model will be generated to prove a suggested hypothesis which is related to one of the two proposed theories about the origin of CoA; concretely, the hypothesis which states that there is a diminished flow in the ArchAo and an increased flow in the ductus arteriosus during early development.

The hypothesis we aim to validate puts forward a diminished flow in the ArchAo and an increased flow in the ductus which will generate an increase in wall shear stress in the distal arch. This increase in WSS will result in a different redistribution of cells in the ArchAo, changing the shape of the arch trying to decrease the WSS. [8] This change of shape to overcome the increased WSS is thought to be one of the origins of the coarctation.

### 3. MARKET ANALYSIS

Coarctation of the aorta is the primarily established application of this proposed CFD model. The model is developed with the aim to improve the understanding of clinicians regarding this condition so the diagnosis and prognosis of this malformation can be improved. An analysis of the global market of clinical prenatal CFD models for CoA is carried out in this section.

#### 3.1. Market drivers

According to the World Health Organization (WHO), cardiovascular diseases are the leading cause of death worldwide. It is reported that every year more people die from a cardiovascular disease than from any other cause. Cardiovascular diseases are a group of disorders of the heart and blood vessels which include congenital heart diseases, which are malformations of the heart present from birth. [26] CoA is the fifth or sixth most common CHD, accounting for 5-8% of neonates with congenital heart diseases. It is reported that the incidence of CoA is one per 2500 births. [27]

Despite advances in fetal echocardiography, this defect remains the most challenging cardiac diagnosis to be made in fetal and early neonatal life due to the patency of the ductus arteriosus. [5] [6] Although there is evidence to suggest that prenatal diagnosis of this condition improves survival and reduces morbidity by allowing early prevention of ductal constriction, detecting CoA in fetal screening is associated with a high number of false-positive diagnosis. This is because it relies on indirect and nonspecific signs and, even when performed by experts. Echocardiography is often unable to distinguish false- from true-positive cases. [6] This important prevalence of CoA, along with false-positive diagnosis is what drives the market to grow into developing new methods capable of improving the understanding, diagnosis, and prognosis of this malformation.

#### 3.2. Evolution of the market

For good prognosis, as early treatment is associated with lower risks of long-term morbidity and mortality, adequate and timely diagnosis of CoA is crucial. [6] This has enhanced researchers to develop new tools that can be used to understand the cause CoA so it can be better diagnosed by doctors.

To improve the diagnosis of CoA, research has been carried out to determine which combination of cardiac parameters can be obtained prenatally and provide the best prediction of postnatal coarctation of the aorta in fetuses with cardiac asymmetry. A multiparametric scoring system was derived, combining size-based cardiac parameters and gestational age at diagnosis to improve the accuracy of fetal echocardiography for the stratification of the risk of CoA. [6]

However, it is thought that the essential sources of CoA morbidity can be explained on the basis of adverse hemodynamics, as it is proposed in the hemodynamics hypothesis. [28] Recent studies suggest that blood flow quantification can help researchers on gaining understanding of this malformation and improving diagnosis and prognosis.

For this reason, researchers are now emphasizing on developing new methods based on accurate flow quantification. Investigation into the hemodynamic and biomechanical basis of morbidity in CoA is considering recent advances in computational modeling. [29]

Computer modeling complexity regarding CoA has increased from 0D models to 1D models and 3D models. The applications of these extend from estimating certain hemodynamic parameters such as flow distribution and pressure gradient to simulating local flow field and estimating hemodynamic parameters such as WSS. Nowadays, the market combines the three models to obtain all the data which is necessary.

0D models of the fetal blood circulation have been developed to study flow distribution and pressure gradients in CoA. These have been suggested as a good approach for assessing and understanding hemodynamic changes in the circulation in a non-invasive manner.

Nonetheless, CFD has emerged as a useful tool to simulate and model the hemodynamics in human aorta. Computational models are usually built on the structural and flow data from CT and MRI. To understand the hemodynamics of CoA, a model needs to be built based on the geometry of the fetal aortic arch and ductus. This is significantly important because when the baby is born the DA closes and the flow distribution along the aortic arch is completely different. Unfortunately, it is challenging to build a CFD model of CoA because we lack data from human fetuses, since it is technically difficult to obtain adequate images and data by CT or MRI of fetuses in vivo. [24]

Fetal echocardiography has been used widely in clinical practice to screen and diagnose CHD in fetuses. It is the method of choice for diagnosis and assessment of fetal cardiac structure, flow, function, and fetal cardiovascular disease. Recent application of spatio-temporal image correlation (STIC) technology in fetal echocardiography has made it possible to acquire 3D/4D gray scale and Doppler images and data in fetuses. This has permitted Zhuo Chen et al to put forward an approach to establish a model of aortic and ductal arch flow in human fetuses using 3D/4D STIC and CFD. The study intends to investigate the hemodynamics of the aortic and ductal flow in normal and simulated CoA; and to explore the implications of the hemodynamic variables in pathophysiology and diagnosis of CoA. [24]

Since predicting critical neonatal coarctation of the aorta before birth is notoriously challenging with a high false positive rate using fetal echocardiography alone. Recent advances in prenatal cardiac magnetic resonance imaging have allowed for the generation of reliable, high-resolution 3-dimensional imaging of the fetal vasculature, as well as to measure vascular flows. A study carried out by David F.A. Lloyd et al applied these novel magnetic resonance imaging techniques to assess fetal vascular morphology and flows in fetuses with suspected CoA. Results showed that reduced blood flow through the left heart was seen in both the true positive and false positive cases when compared to healthy controls. This can be associated with important configurational changes at the aortic isthmus in fetal life, predisposing to CoA when the arterial duct closes after birth. The study suggests that fetal cardiac magnetic resonance imaging may have an important complementary role to fetal echocardiography in predicting neonatal coarctation. [30]

### 3.3. Future perspectives of the market

Although research is being carried out in this field, computational tools have not been established yet as a diagnosis tool for CoA. Despite that the study conducted by Zhuo Chen et al has demonstrated that it is feasible to use 3D/4D STIC techniques to build a 3D model and simulate the flow field in the aortic and ductal arches in normal fetuses and simulated coarctation of aorta, further investigation needs to be done in this field. Future research that could be conducted in the topic could be related to the model of fetuses with various types and severity of coaction of the aortic isthmus to gain insight into the causes and physiology of coarctation of the aorta. Further technological improvement in temporal and spatial resolution of 3D/4D STIC may provide more accurate and quantitative structural and flow data to gain mechanistic insight into the coarctation of the aorta. [24]

Moreover, novel fetal MRI techniques may have a role in both understanding and accurately predicting severe neonatal CoA. However, recent innovations in fetal MRI reconstruction methods may improve imaging in this area and allow for more detailed 3D reevaluation of the great vessels closer to the heart. Additionally, the findings in the article conducted by David F.A. Lloyd et al is based only on preliminary observational data from novel fetal MRI techniques, combined for the first time in vivo. It is thought that expansions of this method based on MRI, may provide an even more sophisticated manner of assessment, including fully spatiotemporally resolved volumes of the beating fetal heart. [30]

## 4. EXECUTION CHRONOGRAM

### 4.1. Work Breakdown Structure (WBS)

A work breakdown structure is used to decompose the project's total scope, including all specific tasks that need to be carried out. This helps with creating a phased schedule of tasks and managing each phase.

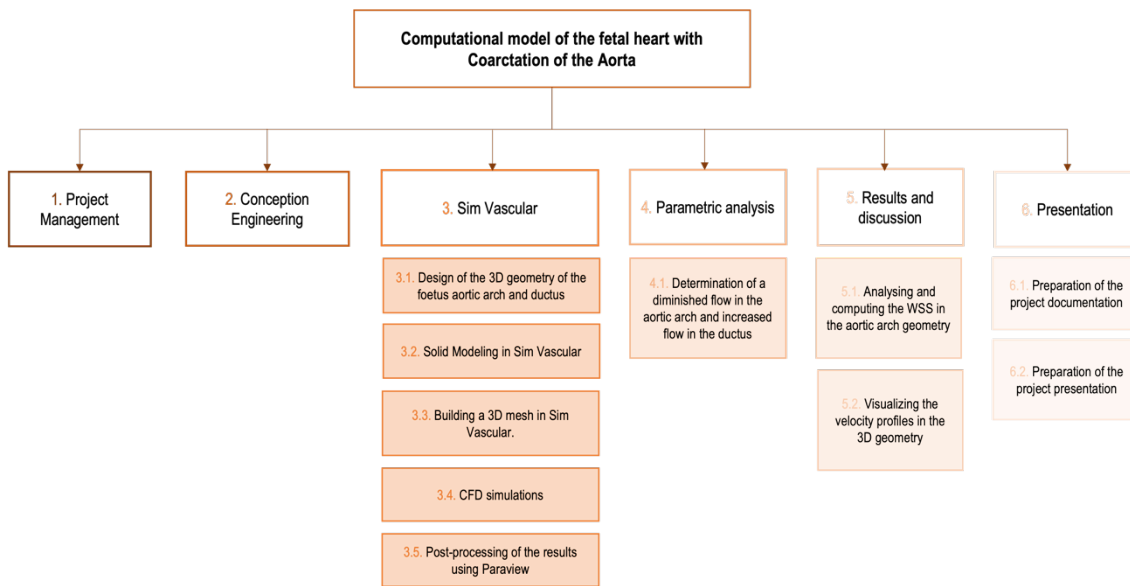


**Figure 5.** EDT diagram

In Figure 5 the work breakdown structure of this TFG can be seen. It lays out everything that the project must accomplish and organizes the tasks into multiple layers displaying the elements graphically. The diagram is useful for the author to organize all the tasks that need to be fulfilled.

### 4.2. Execution Chronogram of the global project (GANTT)

The temporal situation of this project is colored in yellow and comprises the tasks specified in Table 1.

**Table 1.** Tasks involved in this TFG

TASK	DESCRIPTION	START DATE	DURATION (WEEKS)	FINAL DATE
A	Project Management	31 <sup>st</sup> January 2022	20 weeks	17 <sup>th</sup> June 2022



B	Conception Engineering	31 <sup>st</sup> January 2022	2 weeks	14 <sup>th</sup> February 2022
C	Design of the 3D geometry of the fetus aortic arch and ductus	14 <sup>th</sup> February 2022	4 weeks	14 <sup>th</sup> March 2022
D	Solid modeling in Sim Vascular	14 <sup>th</sup> March 2022	1 week	21 <sup>st</sup> March 2022
E	Building a 3D mesh in Sim Vascular	21 <sup>st</sup> March 2022	1 week	28 <sup>th</sup> March 2022
F	CFD simulations	11 <sup>th</sup> April 2022	2 weeks	25 <sup>th</sup> April 2022
G	Post-processing of the results using Paraview	25 <sup>th</sup> April 2022	1 week	2 <sup>nd</sup> May 2022
H	Determination of a diminished flow in the aortic arch and increased flow in the ductus	28 <sup>th</sup> March 2022	2 weeks	11 <sup>th</sup> April 2022
I	Analyzing and computing the WSS in the aortic arch geometry	2 <sup>nd</sup> May 2022	1 week	9 <sup>th</sup> May 2022
J	Visualizing the velocity profiles in the 3D geometry	9 <sup>th</sup> May 2022	1 week	16 <sup>th</sup> May 2022
K	Preparation of the project documentation	16 <sup>th</sup> May 2022	4 weeks	6 <sup>th</sup> June 2022
L	Preparation of the project presentation	6 <sup>th</sup> June 2022	2 weeks	17 <sup>th</sup> June 2022

The timings of the tasks that must be carried out during this TFG are shown in the GANTT execution chronogram in Figure 6.

Task	1st Month				2nd Month				3rd Month				4th Month				5th Month			
	31.1.2022	7.02.2022	14.02.2022	21.02.2022	28.02.2022	7.03.2022	14.03.2022	21.03.2022	28.03.2022	4.04.2022	11.04.2022	18.04.2022	25.04.2022	2.05.2022	9.05.2022	16.05.2022	23.05.2022	30.05.2022	6.06.2022	13.06.2022
A	[Yellow bar from 31.1.2022 to 13.06.2022]																			
B	[Yellow bar from 31.1.2022 to 7.02.2022]																			
C	[Yellow bar from 14.02.2022 to 21.02.2022]																			
D	[Yellow bar from 14.03.2022 to 21.03.2022]																			
E	[Yellow bar from 28.03.2022 to 4.04.2022]																			
F	[Yellow bar from 11.04.2022 to 18.04.2022]																			
G	[Yellow bar from 25.04.2022 to 2.05.2022]																			
H	[Yellow bar from 9.05.2022 to 16.05.2022]																			
I	[Yellow bar from 23.05.2022 to 30.05.2022]																			
J	[Yellow bar from 6.06.2022 to 13.06.2022]																			
K	[Yellow bar from 13.06.2022 to 20.06.2022]																			
L																				[Yellow bar from 20.06.2022 to 27.06.2022]

Figure 6. GANTT diagram of the global project

## 5. CONCEPTION ENGINEERING

This section describes the approaches and methods that will be implemented in the TFG to achieve its objectives. The choice of these proposed solutions is detailed below.

### 5.1. 0D lumped model of the fetal aortic arch

#### a) Input data

The first step was to study what input data needed to be used to build the computational model of the fetal aortic arch and ductus. The input data was obtained from a routine ultrasound scan performed to a healthy pregnant attended in Maternitat Hospital Clinic. Patient-specific blood velocity waveforms from left ventricle and ductus arteriosus were obtained by manual delineation of the envelope of the Doppler blood velocity profiles for one cardiac cycle. Moreover, characteristics of the fetus were given such as the gestational age and estimated fetal weight. The diameter of the left ventricular outflow tract was also obtained from the Doppler images while the diameter for the ductus arteriosus was determined from the literature. [19]

#### b) Design of the 0D model

Once the input parameters for the model were determined, a 0D model of the fetal aortic and ductal arches was designed. The 0D model was constructed using [Simulink](#) from Matlab based on a previous model developed already by the TransCOR group. [7] The 0D or lump-model is based on the Windkessel effect. Arterial segments were modelled with a capacitor, modelling arterial's compliance in parallel to a resistor, modelling blood viscosity and an inductor, modelling blood inertia, as described in Garcia-Canadilla et al. [19] Vascular beds were modelled as a three-element Windkessel model which includes: a proximal resistance  $R_p$  modeling the viscous resistance of the organ, a capacitance  $C$  modeling the organ compliance of downstream vasculature and a distal resistance  $R_d$  modeling the resistance of the capillaries and venous circulation. The 0D model simulations have allowed the author to specify and select what proximal resistance, capacitance and distal resistance parameters describe best the behaviour of the blood in the outlets of the model.

A correct behaviour of the blood flow in the outlets of the model must be ensured. The focus will be set on how the blood flow behaves in the outlets of the model to guarantee that the blood flow in the outlets of the model is as similar as possible to reality. Several simulations were performed to find the values of the vascular beds components (RCR Windkessel parameters) that ensure that that a 30% of the inflow goes to the neck vessels and the upper part of the body and that 70% of the inflow goes through the DescAo to the lower part of the body. These conditions need to be imposed so that blood flow in the fetal aortic arch behaves similarly to real-life. The RCR Windkessel parameters obtained will be then imposed to the outlets in the three-dimensional model. Imposing correct values for the proximal and distal resistance have permitted the author to obtain a similar behavior in the 3D model to the 0D model.

## 5.2. CFD modelling of the fetal aortic arch

To run CFD simulations, Sim Vascular provides a very streamlined process to run blood flow simulations starting from medical images or imported 3D geometries. [21] The Sim Vascular pipeline starts from the user visualization of the imported model to the completion of blood flow simulations and post-processing of simulation results. Figure 7 displays the complete pipeline which needs to be followed to perform the CFD simulations. It starts with the design of the 3D geometry which is then imported to the CFD software and continues with the meshing and all the way through to the post-processing of the simulation results.

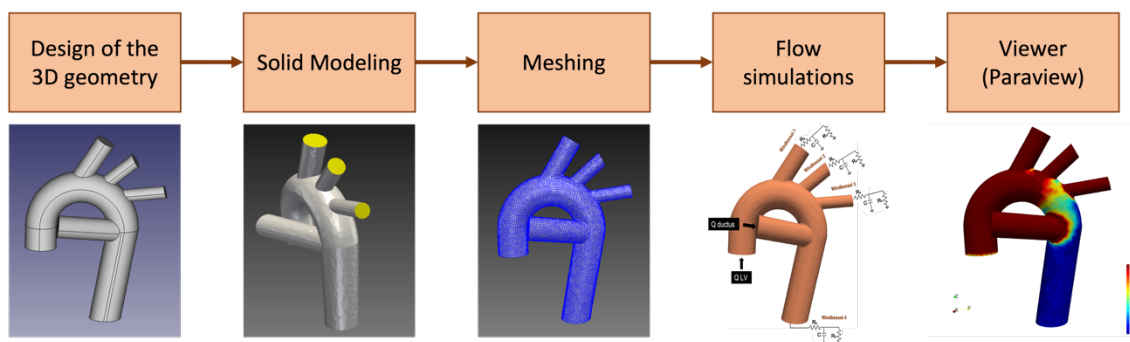


**Figure 7.** The Sim Vascular pipeline leads the user from solid modeling of the imported geometry to completion of blood flow simulations.

### a) Design of the 3D geometry

To design the three-dimensional geometry, the first step is to review what shape and dimensions should be used to model the aortic and ductal arches of a fetus with a gestational age of 34.71 weeks. To determine the shape of the fetal aortic arch the author used the scientific paper [31]. Furthermore, to correctly model the orientation of the neck vessels the author determined that the brachiocephalic artery (BCA) formed an angle of  $45^\circ$  with the tangent of the centerline and the left common carotid (LCCA) and LSA an angle of  $30^\circ$ . To model the diameters of the arteries which are of extremely importance for the simulations, the author used the equations which are described in the paper Garcia-Canadilla et al. [19] The equations were used to determine which was the diameter for the ascending and DescAo, neck vessels and ductus. To build the geometry the author used the software [FreeCAD<sup>3</sup>](#), on the grounds that it was recommended by several professors and that it has a free license.

### b) Solid Modeling

To perform the CFD simulations, the geometry that was created in FreeCAD<sup>3</sup> was imported to Sim Vascular. To do so, FreeCAD<sup>3</sup> and Paraview were used in such a manner to adapt the geometry to Sim Vascular. Furthermore, Sim Vascular was used to refine the geometry in such a way that the meshing could be easily done. In the solid modeling module, the author determined the inlets and outlets of the model, where the boundary conditions were specified.

### c) Building the 3D surface mesh

To do the CFD simulations, the solid model needs to be discretized into small pieces with simple shape, such as triangles or quadrilaterals in two dimensions and tetrahedron or hexahedron in three dimensions. The discretization is necessary to facilitate the numerical solution of partial differential equations in finite-element simulations. The discretized model is a “mesh” and the process of generating discretized model is “mesh generation”. To build the mesh the author chose to use [Sim Vascular](#). Sim Vascular was chosen because the software is developed in a specific and applied easy way which allows users to construct the mesh directly in the software. The meshing tab provided functionality to create a volumetric and surface mesh from the previously imported model for subsequent computational modeling. Sim Vascular supports construction of unstructured tetrahedral meshes as well as several advanced meshing features including boundary surface meshing, radius-based meshing, regional refinement, and adaptive meshing. [32] To generate the mesh, Sim Vascular uses [TetGen](#) which is an open-source mesh generation software using 3D Delaunay Triangulation.

### d) CFD simulations with Sim Vascular

The next step was to carry out the CFD simulations. **Computational fluid dynamics** simulations were used to obtain the numerical solution of the discrete time/space points in the flow field solving the problem by numerical discretization. CFD has been widely used in the field of hemodynamic assessment. To do the CFD simulations, the open-source software Sim Vascular was used. Sim Vascular was chosen because it was strongly recommended by the director and because it has a free license. The software solves the three-dimensional Navier-Stokes equations in an arbitrary domain that it can be represented by a vascular model reconstructed from a medical image or a STL file. Additionally, it provides an efficient finite element flow solver able to simulate physiologic levels. The simulation tab includes three steps, in which a presolver, solver and postsolver are used to generate simulation results. [33] Furthermore, there is functionality to assign boundary condition, material properties, and set parameters for the solver. [32]

### e) Post Processing

The final step was to do a post-processing of the simulation results we obtained. To post process the simulation results of the CFD simulations we chose to use Sim Vascular. This is because, Sim Vascular offers a post-processing module to generate \*.vip and \*.vtu files which extract or calculate relevant hemodynamic quantities such as velocity, pressure, WSS, and oscillatory shear index. [32] These files can be visualized using an open-source scientific visualization software such as [Paraview](#). This platform was chosen because it offers a free license and because it is an open-source, multi-platform, data analysis and visualization application which can be used to quickly build visualizations to analyze simulation data using qualitative and quantitative techniques.

### 5.3. Parametric study: hemodynamical assessment of CoA with different degrees of diminished flow in the aortic arch

A parametric analysis was done to investigate the relationship between flow unbalance and wall shear stress at the isthmus-ductus site. To do the parametric analysis, different blood flow profiles needed to be specified in the inlets of the model. We determined an increasingly prominent blood flow in the ductus which goes from its baseline conditions and increases into a 50%, 60%, 70%, 80% and 90% of flow. This was accompanied by a decreased flow in the ArchAo which decreases from its baseline blood profile to 50%, 40%, 30%, 20% and 10%. To compute the different blood flow profiles, we used [MATLAB R2021a](#) because of personal preference.

## 6. DETAIL ENGINEERING

### 6.1. 0D lumped model of the fetal aortic arch

#### a) Input data

Patient-specific data was used to build the model, including output flow from left ventricle ( $Q_{LV}$ ) and ductus ( $Q_{ductus}$ ), gestational age (GA) and estimated fetal weight (EFW). All the data were obtained from a control fetus. To build the 0D lumped model, the gestational age and the estimated fetal weight of the fetus was used to calculate all the electrical components of the model as described in Garcia-Canadilla et al. [19]

The input of the model was defined by two patient-specific blood-flow inputs  $Q_{LV}$  and  $Q_{DA}$ . Patient-specific blood velocity waveforms from the left ventricular outflow tract and ductus were obtained by manual delineation of the Doppler blood velocity profiles. The delineated velocity for the left ventricular outflow tract and ductus was imported to MatLab. Using equations (1) and (2) patient-specific blood flow inputs (ml/s) were obtained:

$$Q_{LV} = LVOT \cdot \pi \cdot \left( \frac{AoV_{diam}}{2} \right)^2 \quad (1)$$

$$Q_{DA} = Vel_{DA} \cdot \pi \cdot \left( \frac{DA_{diam}}{2} \right)^2 \quad (2)$$

where  $Q_{LV}$  is the inflow in the AscAo,  $Q_{DA}$  is the inflow in the DA,  $AoV_{diam}$  is the diameter of the aortic valve,  $DA_{diam}$  is the diameter of the ductus.

**Table 2.** Data to simulate the 0D lumped model in Simulink

PARAMETERS	DESCRIPTION
Gestational age	34.7100 weeks
Estimated fetal weight (EFW)	2389 g
Heart Rate (HR)	139.8901 bpm
T (period for one cardiac cycle)	0.4584 s

## b) Design of the 0D model

The design for the 0D model was provided from previous work. Four windkessels were modeled in the four outlets of the model to simulate the behavior of blood flow in the fetal ArchAo and DA. Moreover, the windkessel models were used to set the outlet boundary conditions for the CFD simulation in the neck vessels (BCT, LCCA, LSA) and DescAo. The windkessels are modeled using a proximal resistance, distal resistance, and capacitance. The proximal resistance will model the behaviour of the inductance in the lump model, the distal resistance will be modelling the resistance and the capacitance will correspond to the capacitance.

A complete 0D model was built for the blood flow in the ArchAo and ductus and a 0D simulation was carried out obtain the values for the proximal resistance, distal resistance and capacitance which will be used to define the outlet boundary conditions. This is because in the CFD simulations, a RCR boundary condition will be specified in the outlets of the model.

## 6.2. CFD modelling of the fetal aortic arch

### a) Design of the 3D geometry

The first task in this TFG is the design of the 3D geometry. As stated in **CONCEPTION ENGINEERING**, we based our sketch for the ArchAo model on the schematic diagram which can be seen in Figure 8 from the paper “Finite element modelling of pulsatile blood flow in idealized model of human aortic arch: study of hypotension and hypertension”. [31] To model the AscAo, we scaled the length ( $L_1$ ) to a fetus of a gestational age of 34.71 weeks and the ArchAo radius was also scaled from the dimensions which were provided in the scientific paper. [31] The dimensions for the length of the AscAo and the ArchAo radius are summarized in Table 3.

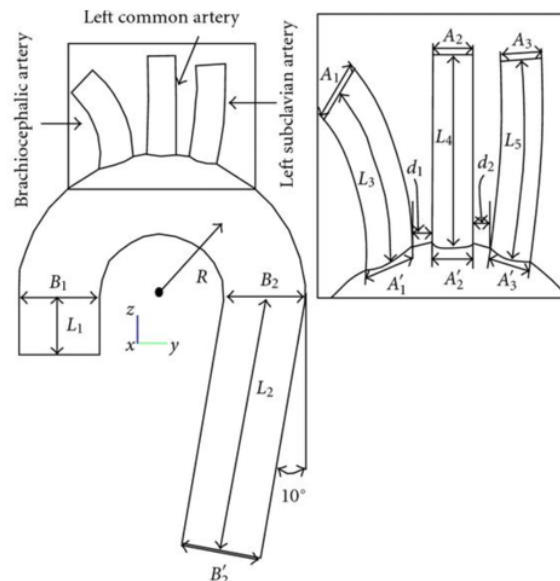


**Figure 8.** Schematic diagram of the 3D aortic arch model. Extracted from [31]



**Table 3.** Artery geometric measures of a fetus

Artery geometric measures (mm)		
AscAo	Length	5.20 mm
ArchAo	Arc radius	9.39 mm

As it is also stated in **CONCEPTION ENGINEERING**, to determine the radius of the neck vessels, AscAo, DA, and DescAo, we used the scientific paper Garcia-Canadilla et al. [19] We were provided this scientific paper which describes the equations used to compute the diameter of the different arterial segments as a function of the gestational age. Table 4 summarizes the values we used to build the geometry. The parameter  $t$  refers to the gestational age of the fetus which is of 34.71 weeks.

**Table 4.** Equations describing the diameter of the different arterial segments of the different of the ArchAo circulation lumped model. Extracted from [19]

Arterial Segment	Radius (mm)	Radius (mm) if $t = 34.71$
AscAo	$\frac{-2.10 + 0.27 \cdot t}{2}$	3.6
DescAo	$\frac{-2.38 + 0.24 \cdot t}{2}$	3.6
DA	$\frac{-2.09 + 0.21 \cdot t}{2}$	2.6
BCA	$\frac{-1.06 + 0.29 \cdot t}{2}$	2.2
LSA	$\frac{-1.22 + 0.12 \cdot t}{2}$	1.7
LCCA	$\frac{-1.52 + 0.14 \cdot t}{2}$	1.5

To design the geometry, we used FREECAD<sup>3</sup>. First, a sketch was designed in two dimensions (2D) to define the constraints. In Figure 9 the sketch for the aortic arch can be seen. We defined that the ArchAo had a radius of 9.39 mm and for the ascending and descending aorta we created two straight lines, 5.17 and 21.68 mm long. Once the sketch was designed, we used the Sweep tool to create a solid shape projected along the paths we sketched.

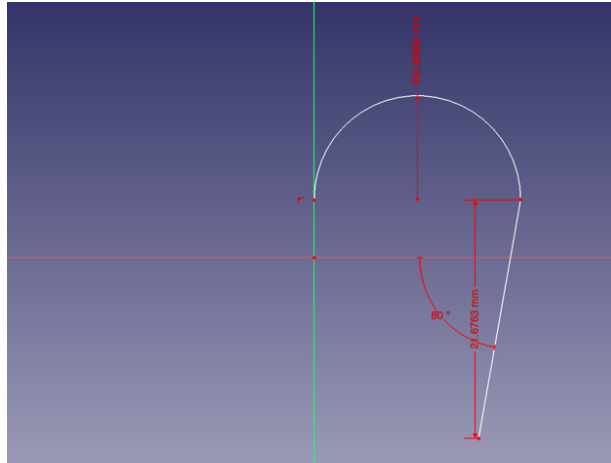


**Figure 9.** Sketch in FREECAD<sup>3</sup> for the aortic arch.

On the other hand, we designed constrained sketches in 2D to define the diameter for each of the arterial segments. Each sketch is designed in a specific plane of the 3D space, so we obtain the geometry we expect. In Figure 10 *left* we can see the outline for each face of the model since the arteries are modeled as solid tubes. To sum up, the Boolean Union tool is used to unify the ArchAo to the four separate segments and create the final geometry.

Among the many sketches designed with FREECAD<sup>3</sup>, the definitive 3D model of the fetal ArchAo and DA is the one in Figure 10 *right*. The final model is the one that best represents the geometry since it shows a slightly more realistic take-off of the neck vessels which are a little pointed according to LV flow.

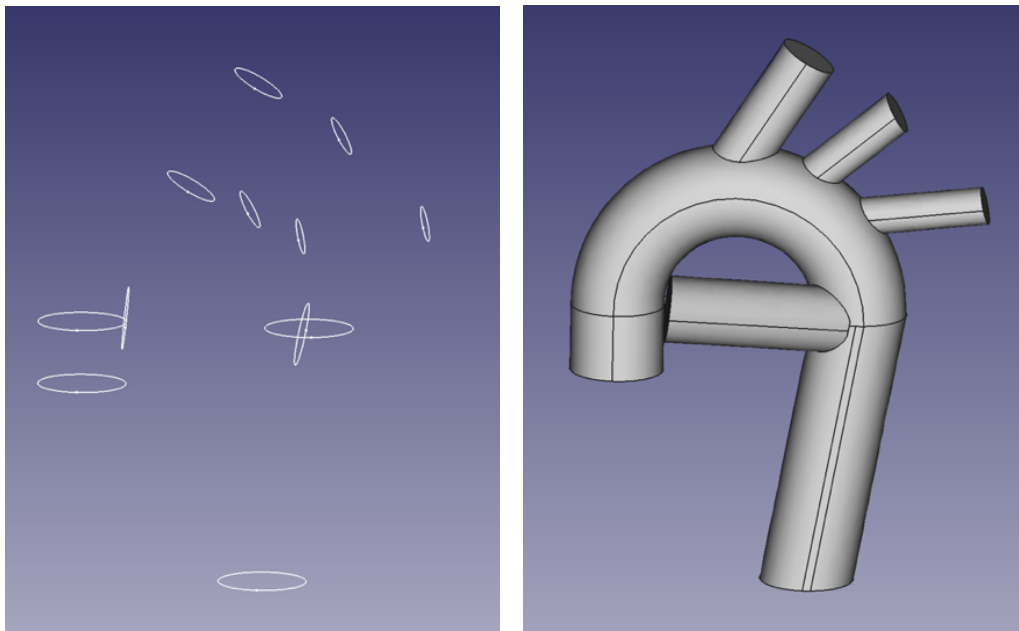


**Figure 10.** *Left*, Sketch in FREECAD<sup>3</sup> of the outlines of the neck vessels, AscAo, DescAo, and DA. *Right*, Final 3D geometry of the fetal arch and ductus designed using FREECAD<sup>3</sup>.

## b) Solid Modeling

The 3D geometry was imported to Sim Vascular. However, before importing a solid geometry to Sim Vascular, a triangulate filter had to be applied using Paraview. The triangulate filter was needed because the data set which was imported from FREECAD<sup>3</sup> was volumetric and contained hexahedrons. Since Sim Vascular only accepts data sets which have a triangulated surface, a triangulate filter had to be applied to decompose polygonal data into only triangles, points, and lines. Having applied the triangulate filter, the geometry will be saved in STL format, and it will be directly imported to the Sim Vascular software. Once the STL file we generated was imported to Sim Vascular (see ANNEX for images), the SV Modeling module allowed users to modify the geometry and adapt it to the software. What is important is that the caps are completely separated from other faces on the surface. To ensure that, we will use the function in the SV Modeling module *Extract Faces*. This function will generate faces (clusters of triangles), based on separation angles between the triangles in the mesh. Applying an extraction angle of 90°, a surface wall for the whole model will be generated. Next, the holes in the model will be filled with seven new surfaces using the tool “*Fill Holes w.IDs*”. At the end of the model creation step, faces of the model are labeled with a user specified name and identifier. These identifiers are important because later are used to specify the boundary conditions in the simulation steps.

Before generating the mesh, the quality of the faces of the model needs to be improved. This is done so the mesh can be generated with no errors in the meshing tab. This can be done by using the remesh tool in the face operations toolbox. A proper value for remesh size will be set for each of the faces. Also, we will apply a local linear subdivision in each of the caps. It is important to mention that for the meshing I had numerous problems because there were many skewed/very small triangles in the surface of my geometry which created an “intersecting facets” problem in the TetGen meshing module. To solve this problem, I had to do a Global Ops remeshing of my geometry with a lower target edge size.

## c) Building the 3D surface mesh

To generate the mesh, we used the SV Meshing module. The mesh is generated from the solid model we created. To generate the isotropic mesh, we had to specify the maximum edge length for a given element for the entire mesh. A global max edge size of 0.528 was specified, resulting in a surface and volumetric mesh with 52459 nodes and 297262 elements as shown in figure. The data of the mesh is detailed in Table 5.

**Table 5.** Mesh statistics

<b>Number of nodes</b>	52459
<b>Number of elements</b>	297262
<b>Number of edges</b>	35016
<b>Number of faces</b>	23344

Also, the mesh generated in Sim Vascular was exported; a \*.vtp file was obtained for the surface mesh and a \*.vtu file for the volumetric mesh. In Paraview, the exported meshes were visualized to check that the \*.vtp file contained the mesh for the surface wall of the model and the caps while the \*.vtu file contained the volumetric mesh of the geometry.

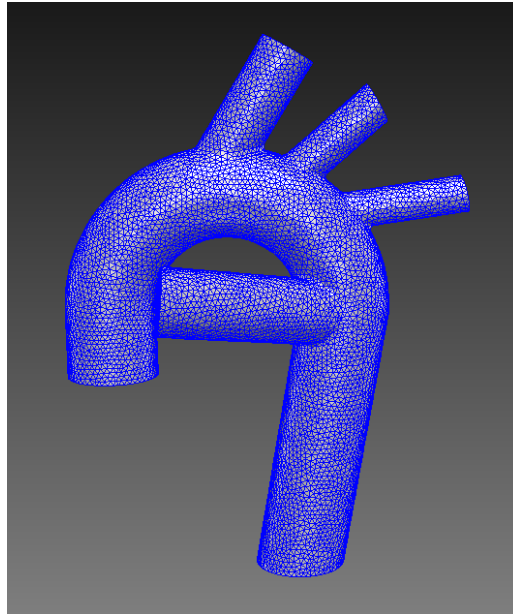


**Figure 11.** 3D Mesh of the ArchAo and DA

#### **d) CFD simulations with Sim Vascular**

The meshing procedure produces an unstructured volumetric mesh that can be used as the computational domain for simulation of blood flow and pressure. [32] Sim Vascular simulation tab includes three steps, in which a preSolver, Solver and postSolver are used to generate the simulation results. [33] The Sim Vascular solver solves incompressible viscous fluid equation on a geometry mesh using finite element algorithm. [32]

To run the simulations, basic parameters had to be specified. These include fluid material properties, and initial conditions. In Sim Vascular, fluid density and viscosity are set as default,  $1.06 \text{ g}\cdot\text{cm}^{-3}$  and  $0.04 \text{ g}\cdot\text{cm}^{-1}\cdot\text{s}^{-1}$ , respectively. Initial pressure was set to “0 mmHg” and initial velocities ( $v_x$ ,  $v_y$ ,  $v_z$ ) were set to be “0 cm/s”. [33] In ANNEX it is shown how the basic parameters are determined.

The boundary conditions are crucial to obtaining high quality simulation results. It is essential that the boundary conditions accurately capture the physiology of vascular networks outside of the 3D domain of the model. Despite the complicated geometrically shape of the fetal ArchAo vascular model we are simulating; its boundary layers can be classified into three distinguished groups. Inflow boundary where a blood flow wave is prescribed; wall boundary which refers to the interface between the vessel wall and the fluid domain, which is assumed to be rigid; and the outlet boundary where a RCR condition is prescribed. [33] It is important that the boundary conditions specified on these surfaces represent the physiology of the vasculature outside the 3D computational domain.

The inlet boundary conditions currently available in Sim Vascular include “prescribed velocities” where users can choose between parabolic, plug, or Womersley velocity profiles. In this study, for the inlet boundary conditions we have imposed a parabolic flow rate  $Q$  (cc/sec) which has been specified in section **Input data**. The blood flow has been specified in a .txt file as shown in *Figure 12*. The first column contains time values and the second column flow values. Another .txt file was generated for the inlet boundary conditions of the AscAo. The flow is negative because Sim Vascular operates in a way that flow coming into the model (forward flow) will have a negative sign, whereas flow coming out of the model (backflow) will be positive.

#	Time (s)	Flow (cc/s)
0.000	-1.8498	
0.001	-2.0726	
0.002	-2.2955	
0.003	-2.5184	
0.004	-2.7520	
0.005	-2.9877	
0.006	-3.2234	
0.007	-3.5524	

**Figure 12.** Inlet boundary condition for the first seven timesteps in the ductus

For the outlets of the ArchAo, we will set a resistance-capacitance-resistance (RCR) model based on the Windkessel effect. The RCR model seen in *Figure 13* allows simulating opposing pressure at the outlet boundary due to downstream resistance from wall shear stress. This condition uses a reduced-order model of the downstream vasculature, considering an electric circuit analog. In this theory, the behavior of the vasculature is represented by three parameters: a proximal resistance  $R_p$ , a capacitance  $C$ , and a distal resistance  $R_d$ . [33]

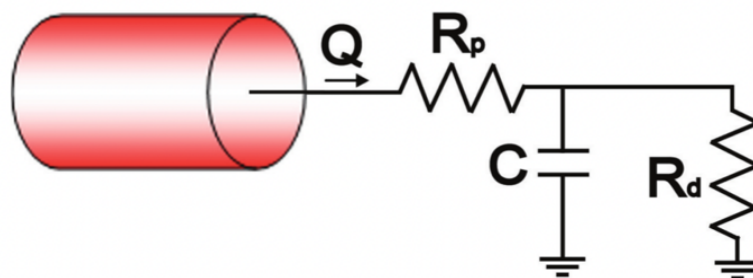


**Figure 13.** Circuit representation of RCR block. Extracted from [33]

The RCR lumped parameters we impose in the outlets of the model are summarized in Table 6. These parameters were obtained from the 0D lumped model simulations which were explained in detail in section **Design of the 0D model**.

**Table 6.** RCR lumped parameters

	$R_p$ (dyn·s/cm <sup>2</sup> )	$R_d$ (dyn·s/cm <sup>2</sup> )	$C$ (cm <sup>2</sup> /dyn)
BCA (Windkessel 1)	1266.35	24217.74	0.0000046
LCCA (Windkessel 2)	1266.35	24217.74	0.0000046
LSA (Windkessel 3)	1266.35	24217.74	0.0000046
DescAo (Windkessel 4)	153	3481.175	0.00000645

In figure 14 it can be seen a diagram of the computational model with the inlet and outlet boundary conditions we have imposed. Four Windkessel are modelled in the outlets of the model, which are the BCA, LCCA, LSA and DescAo, whereas in the inlets of the model we impose a blood flow profile in cc/sec.

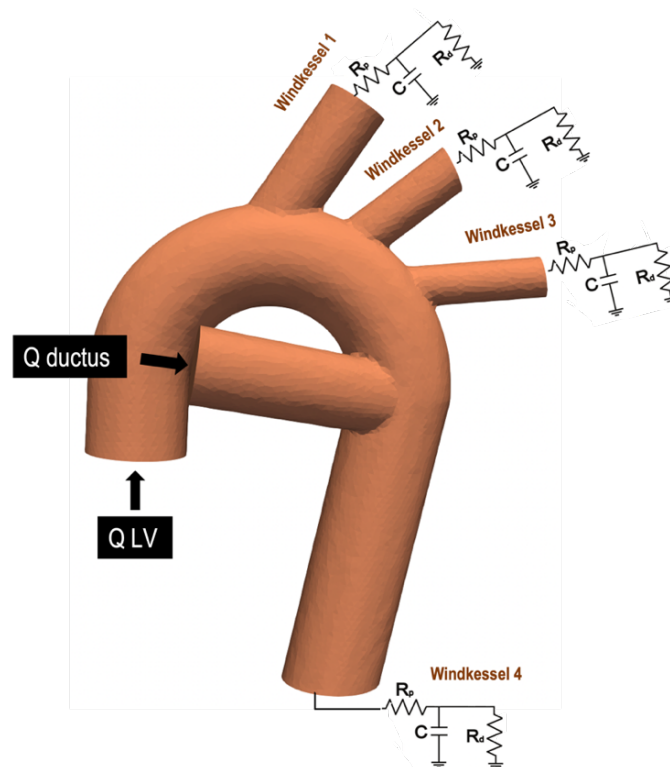


**Figure 14.** CFD model for the fetal ArchAo and DA.

*Figure 15* illustrates a summary of all inlet and outlet boundary conditions we have imposed in the computational model. It is a screenshot obtained from the Simulation module in Sim Vascular. In **ANNEX** you can find screenshots of the whole simulation tab, showing which parameters were imposed in the software to run the simulations.

Inlet and Outlet BCs			
	Name	BC Type	Values
1	ascending	Prescribed Velocities	Assigned
2	ductus	Prescribed Velocities	Assigned
3	descending	RCR	153 0.00000645 3481.175
4	art3	RCR	1266.35 0.0000046 24217.74
5	art2	RCR	1266.35 0.0000046 24217.74
6	art1	RCR	1266.35 0.0000046 24217.74

**Figure 15.** Inlet and Outlet boundary conditions in Sim Vascular.

Moreover, the wall of the vessels was modelled as a rigid surface and no-slip boundary conditions were applied on the vessel wall. In ANNEX it can be seen how we have specified a rigid wall in the model.

To run the simulation, we have had to define various solver parameters. In ANNEX, a table shows all the solver parameters which needed to be specified in order to run the CFD simulations.

**Number of Timesteps:** 458

**Time Step Size:** 0.001

**Number of Timesteps between Restarts:** 1

**Step Construction:** 4

The number of timesteps and time step size control the amount of physical time that you run your problem for. In this case,

$$\text{Total physical time} = N. \text{ time steps} \times \text{Time Step Size} = T$$

Given that the author intends to run the CFD simulations for one cardiac cycle, and the period is 0.458 s, the number of timestep was determined to be 458 and the time step size 0.001. Thus, the total physical time of the simulation is 0.458 s.

### e) Post Processing

Paraview offers a great number of filters which can be applied to the simulation converted files in order to visualize the results we are expecting. The author has centered on visualizing what the velocity magnitude and its direction in the CFD model is. The Stream Tracer filter has helped the author to see the redistribution of flow in the model when there is an imbalanced flow between the DA and the AscAo. The Stream Tracer filter is used because it generates streamlines in the velocity vector field. It enables users to visualize the velocity streamlines in the 3D geometry and see what the magnitude of the velocity during the whole cardiac cycle is.

The Glyph filter was also used to visualize the magnitude and direction of the velocity vector. The filter produces a glyph at each point of the input data set, and it is used to observe the direction and magnitude of the velocity at each point. The filter generates a glyph with arrows, which are oriented and scaled by the input point-centered velocity vector. The Glyph filter is combined with the Volume Rendering filter to give us a better interpretation of what is the magnitude and direction of the flow at each point of the geometry.

Moreover, the author has applied the Temporal Statics Filter to compute the maximum and average value for the wall shear stress during one cardiac cycle. This filter will allow us to evaluate in what parts of the 3D model there is maximum WSS.

### 6.3. Parametric study: hemodynamical assessment of CoA with different degrees of diminished flow in the aortic arch

To investigate the relationship between flow unbalance and wall shear stress at the isthmus-ductus, a parametric analysis has been carried out. We will impose an imbalanced flow in the ductus and ArchAo to study how the flow influences the wall shear stress in the aortic isthmus.

A first simulation will be done imposing a blood-flow profile which corresponds to baseline conditions (Figure 16).

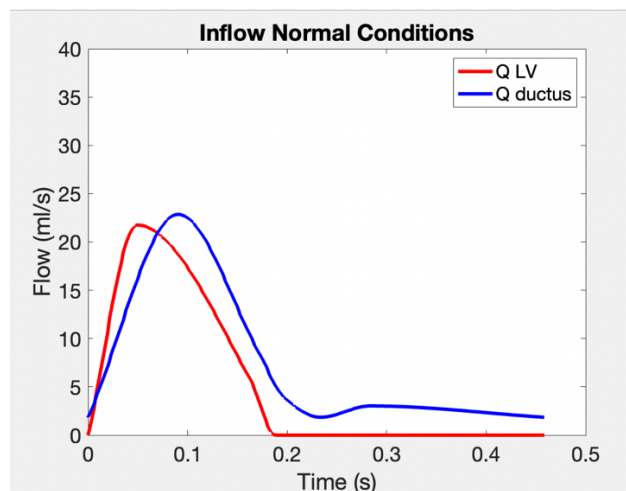


**Figure 16.** Inflow profile for baseline conditions.

From the blood-flow profile in Figure 16, a K factor is obtained for both the AscAo and DA. The K factor will determine which percentage of flow goes through the AscAo and ductus in baseline conditions. To determine the factor, we compute the area under the curve for the left ventricle and ductus and we divide it by the total area. In ANNEX the code in MATLAB can be checked to see how the factors have been computed. Having done that we obtain that the factor for the DA ( $K_{ductus}$ ) is 0.59 and for the AscAo ( $K_{LV}$ ) is 0.41. It can be noticed that there is a slight dominance of the ductus over the AscAo which is what happens in normal conditions in a fetus.



Hereinafter, to model the increasingly prominent flow unbalance the author has multiplied the baseline blood-flow profiles in the left ventricle and ductus by a specific factor. The factor depends on the percentage of flow which had to be imposed in each of the inlets. The six different factors were computed in a MatLab script which can be seen in ANNEX. To compute the different factors, we had to divide the percentage of flow we wanted to impose in the each of the inlets by the specified factor in baseline conditions. This had to be done to maintain the total cardiac output in the model. The computer factors are shown in Table 7.

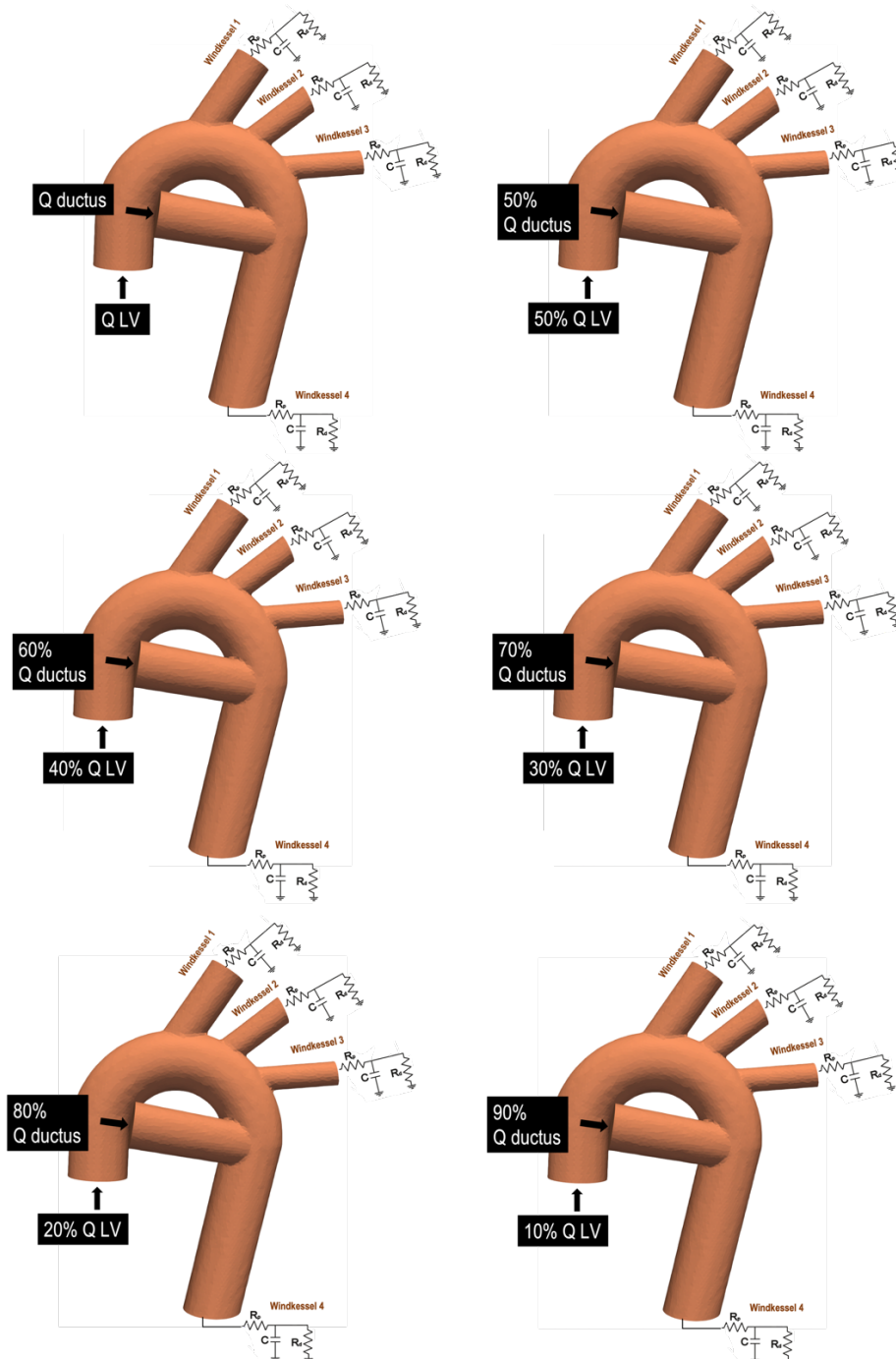


**Figure 17.** Representation of the different degrees of diminished flow in the ArchAo and increased flow in the DA simulated.

**Table 7.** Computed factors to model a diminished flow in the AscAo accompanied by an increased flow in the DA.

	AscAo	DA
Baseline flow profile	$K_{LV} = 0.41$	$K_D = 0.59$
50% DA and 50% AscAo	$K_{LV\_50} = 0.5/ K_{LV}$	$K_{D\_50} = 0.5/K_D$
60% DA and 40% AscAo	$K_{LV\_40} = 0.4/ K_{LV}$	$K_{D\_60} = 0.6/K_D$
70% DA and 30% AscAo	$K_{LV\_30} = 0.3/ K_{LV}$	$K_{D\_70} = 0.7/K_D$
80% DA and 20% AscAo	$K_{LV\_20} = 0.2/ K_{LV}$	$K_{D\_80} = 0.8/K_D$
90% DA and 10% AscAo	$K_{LV\_10} = 0.1/ K_{LV}$	$K_{D\_90} = 0.9/K_D$

Figure 18, Figure 19 and Figure 20 show the plots the author generated when the specified factor for the ductus multiplies the blood flow vector of the ductus and the factor for the AscAo multiplies the corresponding blood flow vector. The figures illustrate how the ductus flow increases progressively and the aortic arch flow is decreased proportionally to maintain the CO. The flow profiles which have been plotted have been downloaded into a .txt file which will be imposed in the inlets of the CFD model for the parametric study.

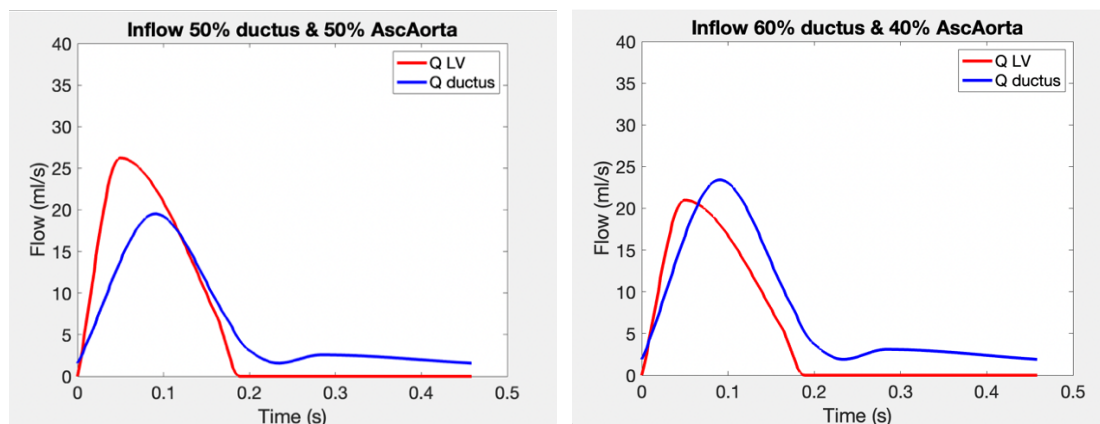


**Figure 18.** Left, 50% aortic flow and 50% ductal flow. Right, 40% aortic flow and 60% ductal flow.

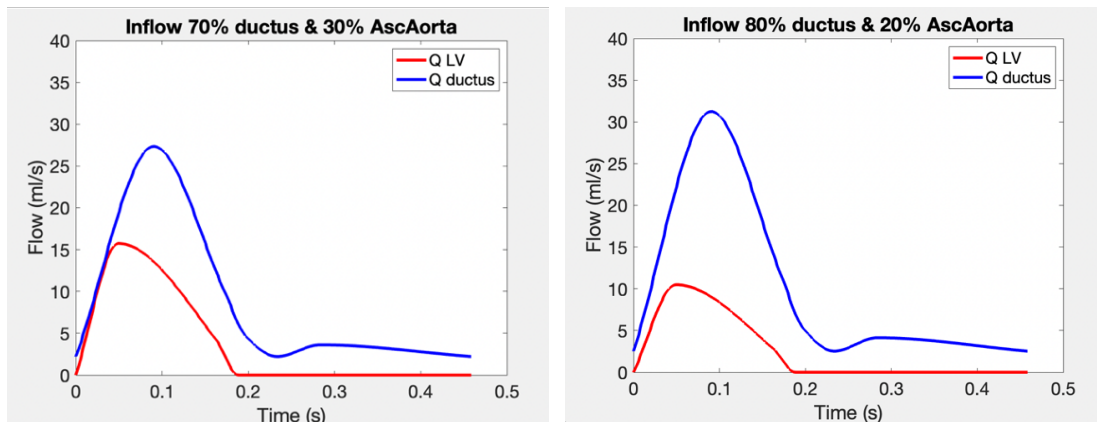


**Figure 19.** *Left*, 30% aortic Flow and 70% ductal flow. *Right*, 20% aortic flow and 80% ductal flow.

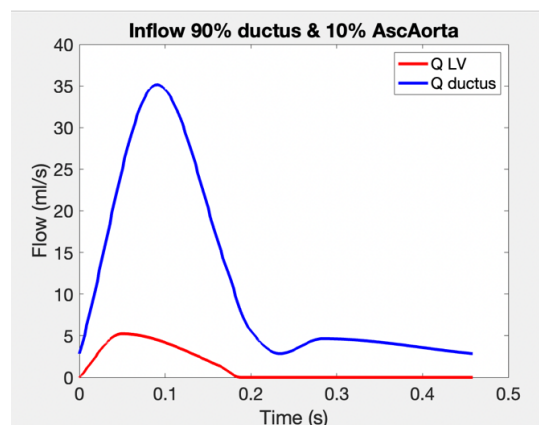


**Figure 20.** 10% aortic flow and 90% ductal flow.

Six blood flow simulations (as in Figure 17) were carried out for the six different blood flow profiles we have described. The flow profiles were imposed in the inlets of the CFD model. The parametric study was helpful to evaluate the relation between an increasingly prominent flow in the ductus and a decreased blood flow in the ArchAo and how it influenced the wall shear stress in the aortic isthmus.

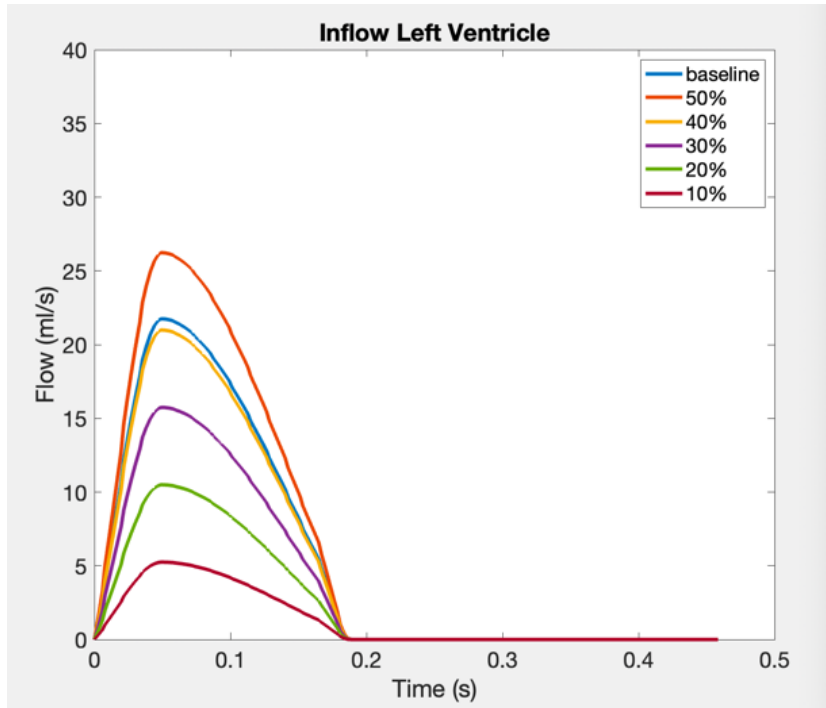


**Figure 21.** Different degrees of diminished flow in the left ventricle.

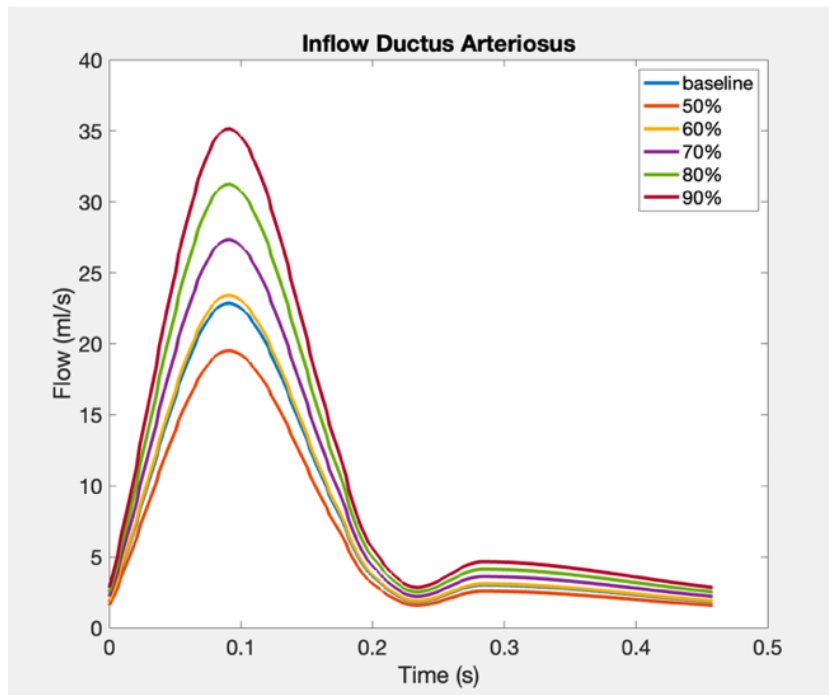


**Figure 22.** Different degrees of increased ductal flow.

## 6.4. Results

The final results of the CFD simulations are shown in Figure 23, 24, 25, 26 and 28. Velocity streamlines and wall shear stress can be clearly seen. The velocity streamlines can be seen together with the velocity magnitude at each point of the model.

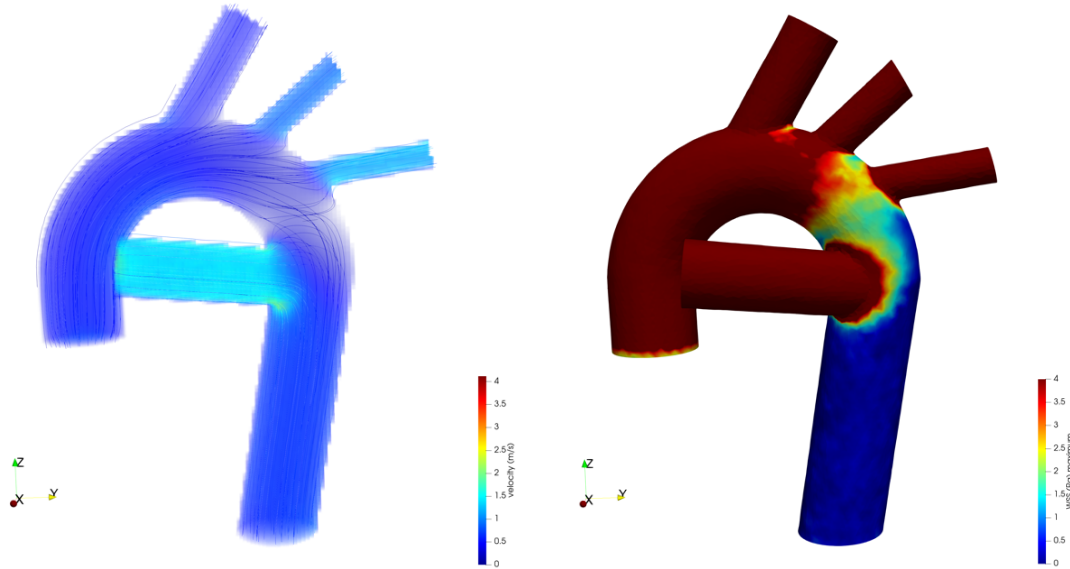


**Figure 23.** Velocity streamlines and WSS in baseline conditions for aortic and ductal flow.

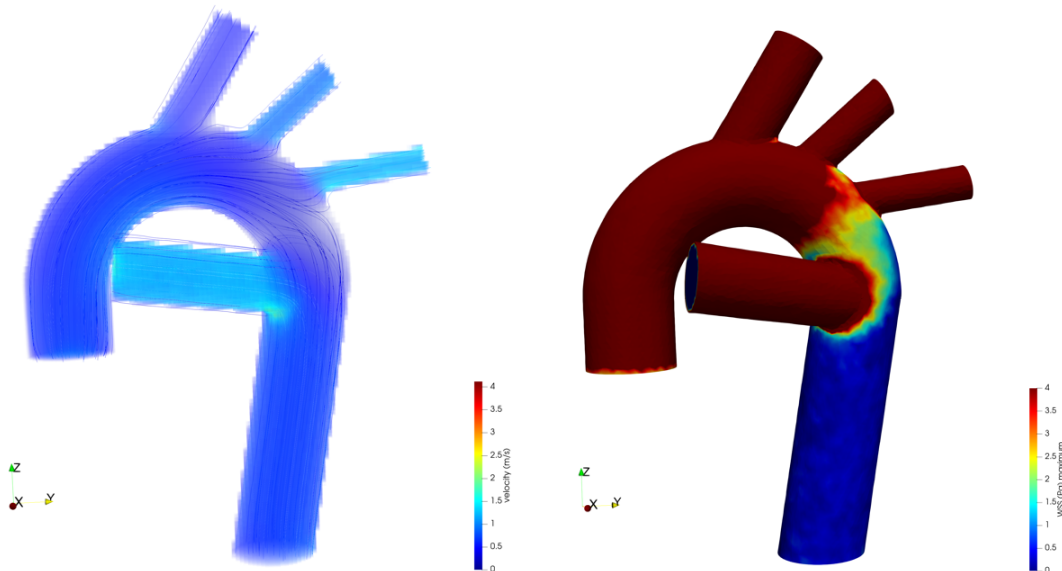


**Figure 24.** Velocity streamlines and WSS with a 50% aortic flow and 50% ductal flow.

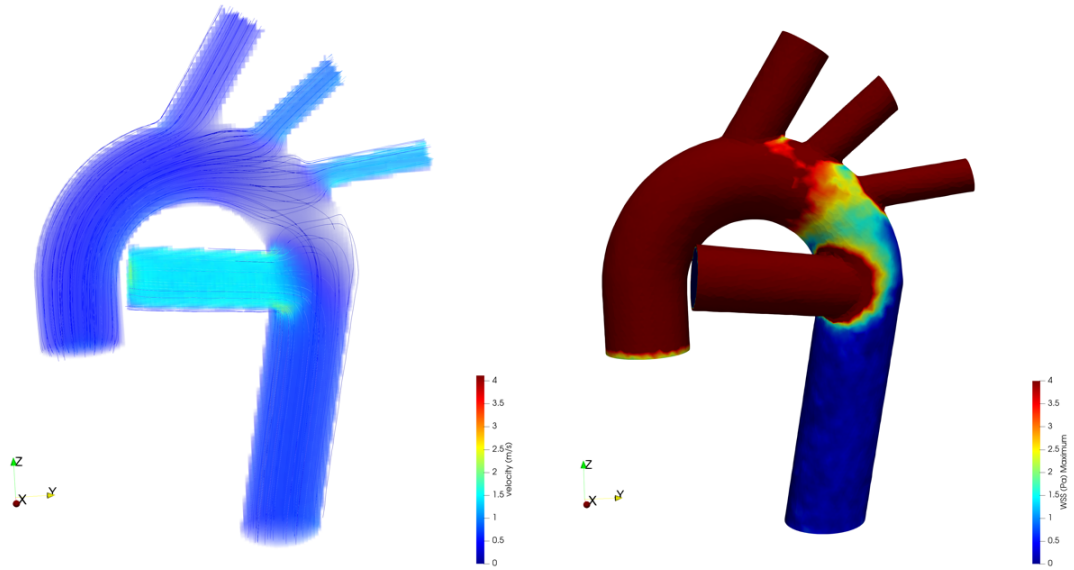


**Figure 25.** Velocity streamlines and WSS with a 40% aortic flow and 60% ductal flow.

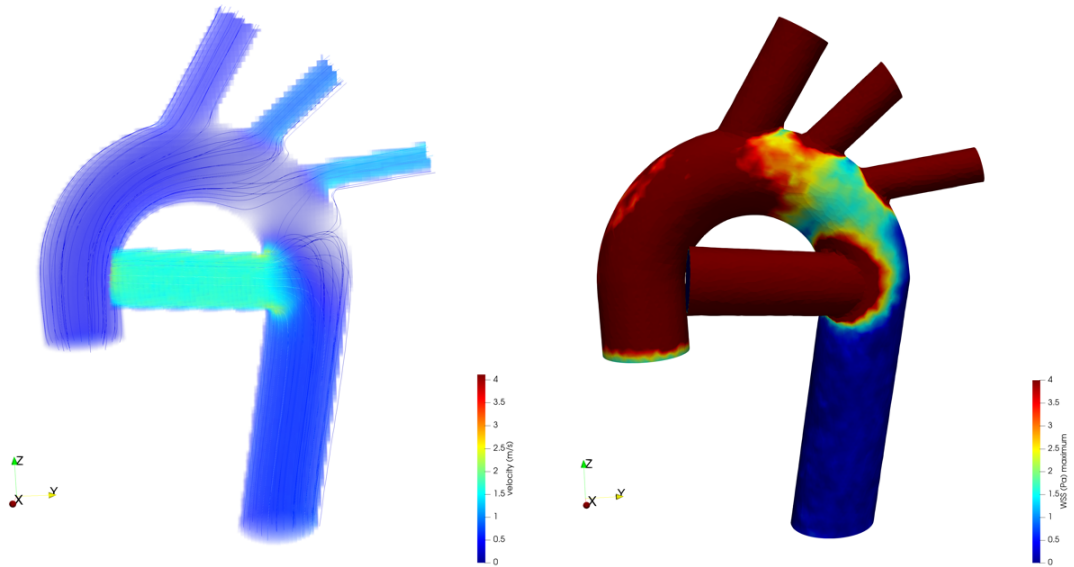


**Figure 26.** Velocity streamlines and WSS with a 30% aortic flow and 70% ductal flow.

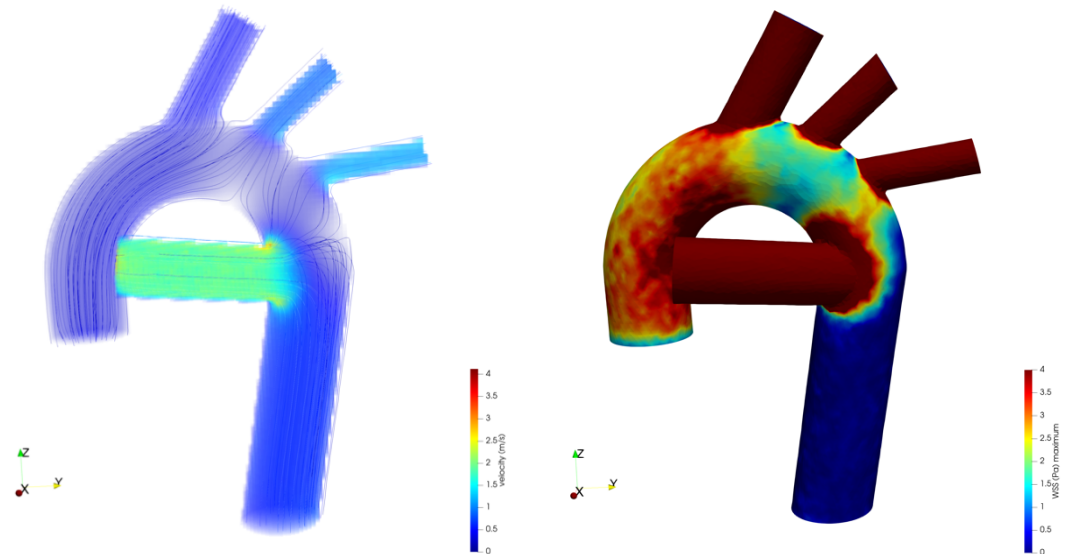


**Figure 27.** Velocity streamlines and WSS with a 20% aortic flow and 80% ductal flow.

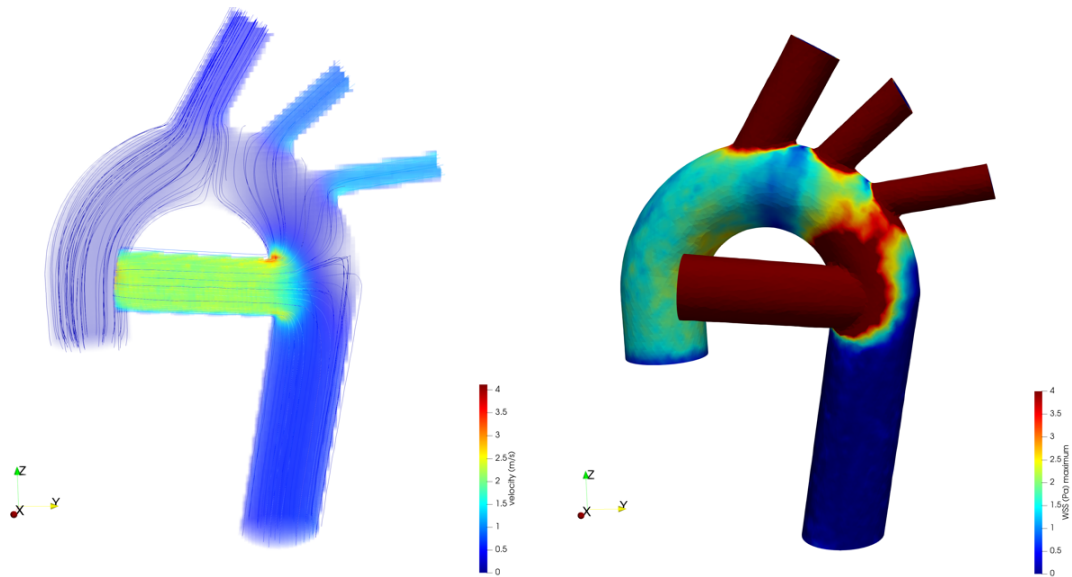


**Figure 28.** Velocity streamlines and WSS with a 10% aortic flow and 90% ductal flow.

As aortic flow diminished from 50% to 10% progressively, velocity and WSS decreased in the AscAo and proximal aortic arch (PAA). However, WSS in the distal aortic arch (DAA) increased with a reduced aortic flow and an increased ductal flow.

In the velocity streamlines representation, we can notice how an increased ductal flow creates a redistribution of flow in the model. It can be seen in Figures 26, 27 and 28 how the streamlines from the ductus inlet go towards the LCCA and LSA, whereas, in Figures 23, 24 and 25 the streamlines in the neck vessels are from the aortic flow. This redistribution of velocity streamlines results in an increased wall shear stress in the DAA when the aortic flow is reduced from 50% to 20%. In Figure 27a slightly increased WSS can be appreciated in the DAA, close to the ductus. However, in Figure 28 we can see how the WSS in the PAA has been reduced significantly, and an increased WSS can be noticed in the distal aortic arch.

Furthermore, the velocity in the aortic isthmus has been reduced with an increased ductal flow because of the redistribution of flow. In Figure 27 and 28 it can be visualized how the number of streamlines in the aortic isthmus is reduced, and some almost zero-flow zones can be noticed in this site as well. Additionally, a second zero-flow zone can be detected in Figure 28 between the left common carotid artery and the left subclavian artery.

## 6.5. Discussion

In this study, a computational model of the fetal aortic arch and ductus was built to simulate pulsatile hemodynamics, including velocity and wall shear stress. This approach can potentially be used to provide insight into the pathophysiology, diagnosis, and assessment of CoA. A diminished aortic flow was imposed accompanied by an increased ductal flow. The results show that reduced blood flow through the left heart is associated with important alterations of flow variables, especially WSS and velocity distribution. The results illustrate important changes in wall shear stress in the distal ArchAo when the aortic flow is notoriously reduced. Moreover, some “zero-flow zones” can be detected in accordance with the increased ductal flow. Results show a “zero-flow zone” in the aortic isthmus when the aortic flow is reduced from 50% to 20% and a second “zero-flow zone” can be seen when the flow in the left ventricle is reduced from 50% to 10%. The “zero-flow zone” at the aortic isthmus can be correlated to the hemodynamics hypothesis on the etiology of CoA which states that there is a reduced flow in the aortic isthmus when there is a diminished flow in the AscAo.

The changing pattern of flow profile, velocity and WSS from the ductal arch to the aortic isthmus may explain the hypothesis that cell migration from the ductal arch to the aortic isthmus of the aorta, which may contribute to the etiology of CoA. As there is more flow unbalance, higher is the WSS in the aortic isthmus, which may impact the receptors in the endothelial cells resulting in a change of shape of the ArchAo and the origin of the coarctation. The increased wall shear stress could be explained with the occurrence of retrograde flow in the distal parts of the take-off of the neck vessels.

Concerning the results obtained, there are possible sources of error that must be considered. Computations were carried out assuming non-mobile rigid walls, which does not capture diastole-systole vascular distension. Moreover, the simulations were performed for only one cardiac cycle, which does not capture the stationary state for the RCR boundary conditions in the outlets of the model. To capture a slightly more realistic blood flow simulation of the fetal circulation in the ArchAo, CFD simulations should be run for more than one cardiac cycle. This approach was not feasible because of it is very computational demanding.

Next step would be to carry out the simulations with a more realistic geometry of the fetal ArchAo simulating the aortic coarctation. The aortic isthmus should be narrowed gradually to study how the WSS changes with a diminished flow when the fetus presents aortic coarctation. Furthermore, control fetuses and fetus with CoA could be used to validate the results.



## 7. TECHNICAL FEASIBILITY: SWOT Analysis

The technical feasibility of the global project is described in the SWOT analysis below (Table 8).

**Table 8.** SWOT analysis of the global project.

Internal Analysis	<h3 style="color: green;">Strengths</h3> <ul style="list-style-type: none"> <li>· High motivation of the author.</li> <li>· Clear definition of the project and its global objectives.</li> <li>· Guidance of top scientists.</li> </ul>	<h3 style="color: red;">Weaknesses</h3> <ul style="list-style-type: none"> <li>· High complexity.</li> <li>· Lack of experience of the authors on the field.</li> <li>· Lack of expertise of the authors on using the required software.</li> <li>· Limited time.</li> </ul>
External Analysis	<h3 style="color: green;">Opportunities</h3> <ul style="list-style-type: none"> <li>· Validation of the proposed hypothesis of the origin of CoA.</li> <li>· Improving our understanding on CoA to improve the diagnosis and prognosis.</li> </ul>	<h3 style="color: red;">Threats</h3> <ul style="list-style-type: none"> <li>· Appearance of published articles aiming to validate the same hypothesis.</li> </ul>

To take maximum advantage of the opportunities and to avoid threats, the confluence of strengths and opportunities and of weaknesses and threats must be evaluated.

The internal strengths of the project must be focused to fit with the opportunities. The author's motivation on the project can be exploited to learn on the field and become an expertise of the required software's. Learning on the field and on the simulation software, was very important to successfully carry out the project. The opportunity, which is the validation of the proposed hypothesis of the origin of CoA, can be chased with the recommendations of the top scientists that support the project. Their expertise and high level of knowledge could be used to successfully carry out the CFD simulations which better reproduced the hemodynamic hypothesis explaining the underlying cause of CoA. Additionally, the second opportunity can be pursued by having a clear definition of the project and its global objectives and by the guidance of top scientists. Knowing what is being demanded, can be positive to the reception of the final CFD model by researchers in the field.

Regarding the threats, they cannot be avoided. However, it was possible to think on strategies to control them and actuate as much as possible, so the consequences are the least damaging possible. The fact that an article is published studying the same effect of a diminished flow in the fetal aortic arch is unavoidable. However, the expertise of the directors is used to think on what the best approach is to follow in order to be able to validate the hypothesis. Moreover, a constant revision of the state of the art of the field is vital to try to avoid the appearance of other published articles on the same topic. Other important weaknesses which should be highlighted is that there was a complete lack of knowledge on the part of the author on how to perform CFD simulations and design 3D geometries. Even so, with the guidance of top scientists and the use of available information on the website it was possible to learn on how to perform the simulations and successfully carry out the project.

## 8. ECONOMICAL FEASIBILITY

The economical cost of the global project is difficult to estimate, given that what not many materials were used. However, an important learning process was necessary to do the CFD simulations.

**Table 9.** Economical cost of the learning process which needed to be done to carry out the global project.

Description	Price
VPH Summer School	50 €
FIMH Virtual Workshop	30 \$
<b>Total Cost</b>	<b>77.99 €</b>

Firstly, it was necessary that the author attended the Virtual Physiological Human (VPH) Summer School, a program which is co-organized by BCN MedTech at the Department of Information and Communication Technologies, Universitat Pompeu Fabra (UPF) and by the Virtual Physiological Human Institute (VPHi), with the collaboration of the UPF department of Experimental and Health Science and the QUAES Foundation. The program provides junior engineers, early researchers, and medical doctors an integrative view of state-of-the-art research for in silico medicine, following a complete pipeline from basic science and clinical needs, to model application. The author took part in a hands-on session about Thrombus formation in Left Atrial Appendage (LAA) in Atrial Fibrillation (AF) patients to learn key methodological and technological concepts about Computational Flow Dynamics. It was mandatory that the author learned what pipeline needed to be followed to perform CFD simulations in order to fulfill the objectives of the project. Although the hands-on session was not focused on blood flow simulations in the fetal ArchAo, it provided a good insight into CFD simulations and how to build surface and volume meshes, as well as how to perform the simulations and visualizing the results. The total cost of the program was 50 € which needs to be taken into account in computing the overall cost of the global project.

Since the author chose to use Sim Vascular to do the CFD simulations, it was necessary to attend a Virtual Workshop focused on new user training. The workshop helped the author on how to use the software package provided in this computational interface. The workshop had a cost of 50 \$ which also needs to be considered when computing the overall cost of the global project.

It is important to highlight that the different software which were used to design the 3D geometry and do the CFD simulations were open-source and free. For this reason, no costs have been associated to the usage of the software. Moreover, since the data we have used to run the simulations was provided to us, no medical equipment and technicians were involved in the project.

Regarding the human resources that participated in the project, a biomedical engineer student was needed to carry out the project and a tutor who would lead and advise the developer. The cost of the student is estimated considering that the annual salary of a junior engineer is approximately 20€/hour. [34] The cost of the tutor was estimated, considering that the annual salary of a senior engineer is 30 €/hour. [35]

**Table 10.** Human resources budget.

Technician	Total time (hours)	Cost (€/hour)	Total Cost (€)
Biomedical engineer student	300	20	6,000
Tutor / Director	12	30	360
<b>Total cost</b>			<b>6,360</b>

Considering the results obtained in the latter tables, it can be approximated a total budget for the project of **6,437.99 €**.

## 9. REGULATION AND LEGAL ASPECTS

Legal aspects were considered during the whole development of the project in order to ensure all time a correct and secure investigation. The global project regulated by the legal aspects provided by Univeristat de Barcelona *Normes generals reguladores dels treballs de fi de grau de la Universitat de Barcelona*. [36]

Given that the project worked with data extracted from a fetus, it is essential to ensure data protection. Data and digital rights are protected under the regulation *Ley Orgánica 3/2018, de 5 de diciembre, de Protección de Datos Personales y garantía de los derechos digitales*. [37] It is also important that the European regulation General Data Protection 2016/679 is satisfied. All data from the Doppler echocardiogram was collected with the appropriate consent from the patients and has been treated anonymously to ensure the intimacy and rights of the patients.

The regulation *Ley 14/2011, de 1 de junio de la Ciencia, la Tecnología y la Innovación* [38] was also followed since it presents some key points for the rights and duties of the researchers in any scientific investigation. This regulation recognized the rights of the researchers by acknowledging their authorship in all the scientific projects that the researcher has contributed.

## 10. CONCLUSIONS AND FUTURE RESEARCH

To conclude, the geometry that has been designed is satisfactory given that it reflects a considerably realistic anatomy of the aortic arch of a fetus. However, there is room for improvement using medical images of Angiogram CT scans. The mesh has been correctly built to run the CFD simulations in Sim Vascular. The CFD simulations have been successfully carried out, simulating a diminished flow in the ArchAo accompanied with an increased flow in the DA. The outlet boundary conditions have correctly been imposed using a RCR Windkessel model, considering that 30% of the inflow goes to the upper body and 70% to the lower body. The parametric analysis has also been done and important conclusions have been drawn which can be seen in the results. Nice visualizations of the simulation data have been captured to analyze the simulation results. Good representation of velocity streamlines could be seen in all simulations and WSS in the isthmus-ductus site of the model could be also computed. The results fit the proposed hypothesis since there is an increase in WSS in the distal aortic arch when we impose a diminished flow in the AscAo. Moreover, a “zero-flow zone” can be detected in the isthmus of the model which matches the hemodynamic hypothesis that decreased flow in the proximal aortic arch leads to a decreased flow in the aortic isthmus.

It is feasible to create a hemodynamic model of human fetal aortic arch using a 3D modeler and CFD tools. However, the geometry is not completely realistic given that it has not been built using CT scans. This has led to the conclusion, that the model we have developed can prove the hypothesis we stated in section [Hypothesis](#) . However, it is important to highlight that the geometry we have designed is ideal. Therefore, to have a more realistic situation, a more real-looking geometry should be built to evaluate more accurately the hypothesis we have previously stated. In the ideal geometry, a redistribution of flow can be observed when the aortic flow is diminished. Additionally, it can be noticed an increase in wall shear stress in the distal aortic arch. Nonetheless, the ideal geometry has permitted the author to accurately study the hemodynamic factors which influence the “flow-dependency” of the fetal ArchAo development but to validate the hypothesis a second phase of the project should be carried out using a non-ideal geometry. First, this non-ideal geometry can be reached by narrowing progressively the diameter of the Aol. This approach has not been carried out due mainly to time constraints. Furthermore, the simulation results gathered from this non-ideal geometry should be then compared to flow simulation in segmented geometries from CT scans of control patients and fetuses with CoA.

All in all, future lines of the project would be to simulate the coarctation, using a geometry with a decreased radius in the isthmus of the aortic arch. Moreover, other future lines would be to use a control real geometry without CoA and a real geometry with CoA to evaluate the WSS in the aortic isthmus to prove if the hypothesis we stated is validated. Other CFD simulations could be carried out to evaluate other types of CoA and different degrees of severity. These simulations could include aortic arch hypoplasia to gain profound perception into the causes and pathophysiology of coarctation of the aorta.

## 11. REFERENCES

- [1] Themes, U. (2016b, January 11). Coarctation of the Aorta. Radiology Key. Retrieved May 22, 2022, from <https://radiologykey.com/coarctation-of-the-aorta-2/>
- [2] Buyens, A., Gyselaers, W., Coumans, A., Al Nasiry, S., Willekes, C., Boshoff, D., Frijns, J. P., & Witters, I. (2012). Difficult prenatal diagnosis: fetal coarctation. *Facts, views & vision in ObGyn*, 4(4), 230–236.
- [3] Utrecht University. (2016). Coarctation of the aorta - Clinical decision making When is the arch too small? <http://www.utrechtsessions.nl/wp-content/uploads/2020/02/Coarctation-When-is-the-aortic-arch-too-small-Damien-Bonnet.pdf>.
- [4] Hoffman, J. I. (2018). The challenge in diagnosing coarctation of the aorta. *Cardiovascular Journal of Africa*, 29(4), 252–255. <https://doi.org/10.5830/cvja-2017-053>
- [5] Toole, B. J., Schlosser, B., McCracken, C. E., Stauffer, N., Border, W. L., & Sachdeva, R. (2015). Importance of Relationship between Ductus and Isthmus in Fetal Diagnosis of Coarctation of Aorta. *Echocardiography*, 33(5), 771–777. <https://doi.org/10.1111/echo.13140>
- [6] Gómez-Montes, E., Herraiz, I., Mendoza, A., Escribano, D., & Galindo, A. (2013). Prediction of coarctation of the aorta in the second half of pregnancy. *Ultrasound in Obstetrics & Gynecology*, 41(3), 298–305. <https://doi.org/10.1002/uog.11228>
- [7] Giménez Mínguez P, Bijmens B, Bernardino G, Lluch E, Soveral I, Gómez O, Garcia-Canadilla P. Assessment of haemodynamic remodeling in fetal aortic coarctation using a lumped model of the circulation. In: Pop M, Wright GA, editors. *Functional Imaging and Modelling of the Heart. 9th International Conference, FIMH 2017, Proceedings. 2017 Jun 11-13; Toronto, Canada.* p. 471-80. (LNCS; no. 10263). DOI: 10.1007/978-3-319-59448-4\_45
- [8] von Kodolitsch Y, Aydin AM, Bernhardt AM, Habermann C, Treede H, Reichenspurner H, Meinertz T, Dodge-Khatami A. Aortic aneurysms after correction of aortic coarctation: a systematic review. *Vasa*. 2010 Feb;39(1):3-16. doi: 10.1024/0301-1526/a000001
- [9] Sobre la recerca | Hospital. (2016). *Clinic Barcelona*. <https://www.clinicbarcelona.org/ca/idibaps/sobre-nosaltres>
- [10] Annual Scientific Report 2018. (2018). *Clinic*. <https://www.clinicbarcelona.org/uploads/media/default/0001/69/e84b11c67b7f37eb24ec922fdffbbf9c25d6ff3f.pdf>
- [11] Dumrongmongcolgul, N., Searles, R.J., Casimir, M.D., Zhu, Q. (2021). Vascular Access and Anesthesia for Patients with Cardiac Anatomic Anomalies. In: Narayan, D., Kapadia, S.E., Kodumudi, G., Vadivelu, N. (eds) *Surgical and Perioperative Management of Patients with Anatomic Anomalies*. Springer, Cham. [https://doi.org/10.1007/978-3-030-55660-0\\_20](https://doi.org/10.1007/978-3-030-55660-0_20)
- [12] Jennifer S. Nelson, Matthew L. Stone, James J. Gangemi. (2019). 45 - Coarctation of the Aorta. In *Critical Heart Disease in Infants and Children (Third Edition)* (pp. 551–5664). Elsevier.

- [13] Fetal Circulation. (2021, May 13). Www.Heart.Org. <https://www.heart.org/en/health-topics/congenital-heart-defects/symptoms--diagnosis-of-congenital-heart-defects/fetal-circulation>
- [14] Morton, S. U., & Brodsky, D. (2016). Fetal Physiology and the Transition to Extrauterine Life. *Clinics in perinatology*, 43(3), 395–407. <https://doi.org/10.1016/j.clp.2016.04.001>
- [15] Galindo, A., Herraiz, I., Escribano, D., Lora, D., Melchor, J. C., & de la Cruz, J. (2010). Prenatal Detection of Congenital Heart Defects: A Survey on Clinical Practice in Spain. *Fetal Diagnosis and Therapy*, 29(4), 287–295. <https://doi.org/10.1159/000322519>
- [16] Allan, L. D., Chita, S. K., Anderson, R. H., Fagg, N., Crawford, D. C., & Tynan, M. J. (1988). Coarctation of the aorta in prenatal life: an echocardiographic, anatomical, and functional study. *Heart*, 59(3), 356–360. <https://doi.org/10.1136/hrt.59.3.356>
- [17] Morgan CT, Mueller B, Thakur V, Guerra V, Jull C, Mertens L, Friedberg M, Golding F, Seed M, Miner SES, Jaeggi ET, Manhiot C, Nield LE. (2019). Improving Prenatal Diagnosis of Coarctation of the Aorta. In *Canadian Journal of Cardiology: Vol. Volume 35, Issue 4* (pp. 453–461). Elsevier. <https://doi.org/10.1016/j.cjca.2018.12.019>
- [18] Crispi F, Valenzuela-Alcaraz B, Cruz-Lemini M, Gratacós E. Ultrasound assessment of fetal cardiac function. *Australas J Ultrasound Med*. 2013;16(4):158-167. doi:10.1002/j.2205-0140.2013.tb00242.x.
- [19] Garcia-Canadilla, P., Rudenick, P. A., Crispi, F., Cruz-Lemini, M., Palau, G., Camara, O., ... Bijens, B. H. (2014). A computational model of the fetal circulation to quantify blood redistribution in intrauterine growth restriction. *PLoS Comput Biol*, 10(6), e1003667. <https://doi.org/10.1371/journal.pcbi.1003667>
- [20] Liu, H., Wang, D., Leng, X., Zheng, D., Chen, F., Wong, L. K. S., Shi, L., & Leung, T. W. H. (2020). State-of-the-Art Computational Models of Circle of Willis With Physiological Applications: A Review. *IEEE Access*, 8, 156261–156273. <https://doi.org/10.1109/access.2020.3007737>
- [21] Yogeswaran, S., & Liu, F. (2021). Vascular flow simulations using SimVascular and OpenFOAM. doi:10.1101/2021.09.11.21263191
- [22] Garcia-Canadilla, P., Crispi, F., Cruz-lemini, M., Triunfo, S., Nadal, A., Valenzuela- alcaraz, B., ... Bijens, B. H. (2015). Patient-specific estimates of vascular and placental properties in growth-restricted fetuses based on a model of the fetal circulation. *Placenta*, 36, 981–989. <https://doi.org/10.1016/j.placenta.2015.07.130>
- [23] Bachelor's Degree Final Project (UPF). (2017, June). Fetal and Neonatal Hemodynamic Assessment of Aortic Coarctation - Imaging and Computational Modelling. Àngels Calvet Mirabent.
- [24] Chen, Z., Zhou, Y., Wang, J., Liu, X., Ge, S., & He, Y. (2017). Modeling of coarctation of aorta in human fetuses using 3D/4D fetal echocardiography and computational fluid dynamics. *Echocardiography*, 34(12), 1858–1866. <https://doi.org/10.1111/echo.13644>



- [25] Chen, Z., Zhao, H., Zhao, Y., Han, J., Do-Nguyen, C. C., Wei, Z., He, Y., & Ge, S. (2020). Abstract 14543: Diminished Aortic Flow in Fetus and Its Implications in Development of Aortic Coarctation and Arch Interruption: A 3d/4d Fetal Echocardiography and Computational Fluid Dynamics Study. *Circulation*, 142(Suppl\_3). [https://doi.org/10.1161/circ.142.suppl\\_3.14543](https://doi.org/10.1161/circ.142.suppl_3.14543)
- [26] Enfermedades cardiovasculares. (2017, May 17). Organización Mundial de la Salud. Retrieved May 29, 2022, from [https://www.who.int/es/news-room/fact-sheets/detail/cardiovascular-diseases-\(cvds\)](https://www.who.int/es/news-room/fact-sheets/detail/cardiovascular-diseases-(cvds))
- [27] Bugeja, J., Cutajar, D., Zahra, C., Parascandalo, R., Grech, V., & DeGiovanni, J. V. (2016). Aortic stenting for neonatal coarctation of the aorta - when should this be considered?. *Images in paediatric cardiology*, 18(3), 1–4.
- [28] Sadeghi, R., Khodaei, S., Ganame, J., & Keshavarz-Motamed, Z. (2020). Towards non-invasive computational-mechanics and imaging-based diagnostic framework for personalized cardiology for coarctation. *Scientific Reports*, 10(1). <https://doi.org/10.1038/s41598-020-65576-y>
- [29] LaDisa, J. F., Alberto Figueroa, C., Vignon-Clementel, I. E., Jin Kim, H., Xiao, N., Ellwein, L. M., Chan, F. P., Feinstein, J. A., & Taylor, C. A. (2011). Computational Simulations for Aortic Coarctation: Representative Results From a Sampling of Patients. *Journal of Biomechanical Engineering*, 133(9). <https://doi.org/10.1115/1.4004996>
- [30] Lloyd, D. F., van Poppel, M. P., Pushparajah, K., Vigneswaran, T. V., Zidere, V., Steinweg, J., van Amerom, J. F., Roberts, T. A., Schulz, A., Charakida, M., Miller, O., Sharland, G., Rutherford, M., Hajnal, J. V., Simpson, J. M., & Razavi, R. (2021). Analysis of 3-Dimensional Arch Anatomy, Vascular Flow, and Postnatal Outcome in Cases of Suspected Coarctation of the Aorta Using Fetal Cardiac Magnetic Resonance Imaging. *Circulation: Cardiovascular Imaging*, 14(7). <https://doi.org/10.1161/circimaging.121.012411>
- [31] Vasava, P., Jalali, P., Dabagh, M., & Kolari, P. J. (2012). Finite Element Modelling of Pulsatile Blood Flow in Idealized Model of Human Aortic Arch: Study of Hypotension and Hypertension. *Computational and Mathematical Methods in Medicine*, 2012, 1–14. <https://doi.org/10.1155/2012/861837>
- [32] Updegrove, A., Wilson, N. M., Merkow, J., Lan, H., Marsden, A. L., & Shadden, S. C. (2016). SimVascular: An Open Source Pipeline for Cardiovascular Simulation. *Annals of Biomedical Engineering*, 45(3), 525–541. <https://doi.org/10.1007/s10439-016-1762-8>
- [33] SimVascular Docs. (2017). Sim Vascular. Retrieved May 15, 2022, from <https://simvascular.github.io/docsFlowSolver.html>
- [34] Castillo, E. (2018, April 10). Analista de datos, el puesto más demandado (y mejor pagado) por las empresas. *Cinco Días*. Retrieved June 5, 2022, from [https://cincodias.elpais.com/cincodias/2018/04/09/midinero/1523274767\\_631043.html](https://cincodias.elpais.com/cincodias/2018/04/09/midinero/1523274767_631043.html)
- [35] BOLETÍN OFICIAL DEL ESTADO. (2019, May). MINISTERIO DE TRABAJO, MIGRACIONES Y SEGURIDAD SOCIAL.

- [36] Grau en Enginyeria Biomedica - Facultat de Medicina i Ciències de la Salut - Universitat de Barcelona. (2017, June 7). Universitat de Barcelona. Retrieved June 5, 2022, from <https://www.ub.edu/portal/web/medicina-ciencies-salut/grau//ensenyament/detallEnsenyament/4917593/10>
- [37] BOE.es - BOE-A-2018-16673 Ley Orgánica 3/2018, de 5 de diciembre, de Protección de Datos Personales y garantía de los derechos digitales. (2018, December 6). Agencia Estatal Boletín Oficial del Estado. Retrieved June 5, 2022, from <https://www.boe.es/buscar/act.php?id=BOE-A-2018-16673>
- [38] BOE.es - BOE-A-2018-16673 Ley Orgánica 3/2018, de 5 de diciembre, de Protección de Datos Personales y garantía de los derechos digitales. (2018, December 6). Agencia Estatal Boletín Oficial del Estado. Retrieved June 5, 2022, from <https://www.boe.es/buscar/act.php?id=BOE-A-2018-16673>

## 12. ANNEX

### 12.1. MatLab code

```
%% Load input parameters
load('InputData.mat')
GA = Data.GA; % weeks %age fetus
HR = Data.HR; % (bpm) %heart rate
T = Data.T; % cycle durayion (s)
W = Data.EFW; % estimated fetal weight
W0 = 10^(0.2508 + 0.1458*GA -0.0016*GA^2); % theoretical estimated
fetal weight
KWeight = (W/W0)^0.33;

%% Calculate nominal parameters

Set_initial_parameters %Initialization of all the parameters

%% Open input function

LVOT = Data.Vel_LVOT_real';
Vel_DA = Data.Vel_DA';
AoV_diam = Data.DiamAoV; % (mm)
DA_diam = 5.2; % (mm)
Q_LV = LVOT * pi * (AoV_diam*1E-1/2)^2;
Q_ductus = Vel_DA* pi * (DA_diam*1E-1/2)^2;

dt = Data.dt;
Qi.signals.values = Q_LV;
Qductus.signals.values = Q_ductus;
Qi.time = [];
Qductus.time = [];
time = linspace(0, Data.T, numel(Qi.signals.values));

%% Simulation parameters

N_SAMPLES_CYCLE = numel(Qi.signals.values);
tstep=Data.dt;
beats=25;
Tend=(N_SAMPLES_CYCLE*beats-1)*dt;

load_system('geometria_fetal.mdl');
hAcs = getActiveConfigSet(gcs);
hAcs.set_param('StopTime', num2str(Tend));

myobj =
sim('geometria_fetal.mdl', 'SrcWorkspace', 'Current', 'StopTime', num2str(
Tend));

%% Initial simulation

area_QLV = sum(Q_LV.*dt); %ml
area_Qductus = sum(Q_ductus.*dt); %ml

area_inlet_flow = area_QLV + area_Qductus; %ml

K_LV = area_QLV/area_inlet_flow;
K_D = area_Qductus /area_inlet_flow;
```

```

%% 50% QLV and 50% ductus
Q_LV_5050 = Q_LV.*(0.5/K_LV);
Q_ductus_5050 = Q_ductus.*(0.5/K_D);

%% 40% QLV and 60% ductus
Q_LV_6040 = Q_LV.*(0.4/K_LV);
Q_ductus_6040 = Q_ductus.*(0.6/K_D);

%% 30% QLV and 70% ductus
Q_LV_7030 = Q_LV.*(0.3/K_LV);
Q_ductus_7030 = Q_ductus.*(0.7/K_D);

%% 20% QLV and 80% ductus
Q_LV_8020 = Q_LV.*(0.2/K_LV);
Q_ductus_8020 = Q_ductus.*(0.8/K_D);

%% 10% QLV and 90% ductus
Q_LV_9010 = Q_LV.*(0.1/K_LV);
Q_ductus_9010 = Q_ductus.*(0.9/K_D);

%% Plot the figures
figure(1)
plot(time,Q_LV,'LineWidth',3,'Color','#0072BD'); hold on;
plot(time,Q_LV_5050,'LineWidth',3,'Color','#D95319'); hold on;
plot(time,Q_LV_6040,'LineWidth',3,'Color','#EDB120'); hold on;
plot(time,Q_LV_7030,'LineWidth',3,'Color','#7E2F8E'); hold on;
plot(time,Q_LV_8020,'LineWidth',3,'Color','#77AC30'); hold on;
plot(time,Q_LV_9010,'LineWidth',3,'Color','#A2142F')
ylim([0 40]);
xlabel('Time (s)');
ylabel('Flow (ml/s)');
legend("baseline", "50%", "40%", "30%", "20%", "10%")
set(gca,'FontSize',18.0)
title("Inflow Left Ventricle")

figure(2)
plot(time,Q_ductus,'LineWidth',3,'Color','#0072BD'); hold on;
plot(time,Q_ductus_5050,'LineWidth',3,'Color','#D95319'); hold on;
plot(time,Q_ductus_6040,'LineWidth',3,'Color','#EDB120'); hold on;
plot(time,Q_ductus_7030,'LineWidth',3,'Color','#7E2F8E'); hold on;
plot(time,Q_ductus_8020,'LineWidth',3,'Color','#77AC30'); hold on;
plot(time,Q_ductus_9010,'LineWidth',3,'Color','#A2142F')
ylim([0 40]);
xlabel('Time (s)');
ylabel('Flow (ml/s)');
legend("baseline", "50%", "60%", "70%", "80%", "90%")
set(gca,'FontSize',18.0)
title("Inflow Ductus Arteriosus")

%% Plot the figures
figure(3)
plot(time,Q_LV,'LineWidth',3,'Color','r')
hold on;
plot(time,Q_ductus,'LineWidth',3,'Color','b')
ylim([0 40]);
xlabel('Time (s)');
ylabel('Flow (ml/s)');
legend("Q LV", "Q ductus")
set(gca,'FontSize',18.0)
title("Inflow Normal Conditions")

```

```

figure(4)
plot(time,Q_LV_5050,'LineWidth',3,'Color','r')
hold on;
plot(time,Q_ductus_5050,'LineWidth',3,'Color','b')
ylim([0 40]);
xlabel('Time (s)');
ylabel('Flow (ml/s)');
legend("Q LV", "Q ductus")
set(gca,'FontSize',18.0)
title("Inflow 50% ductus & 50% AscAorta")

```

```

figure(5)
plot(time,Q_LV_6040,'LineWidth',3,'Color','r')
hold on;
plot(time,Q_ductus_6040,'LineWidth',3,'Color','b')
ylim([0 40]);
xlabel('Time (s)');
ylabel('Flow (ml/s)');
legend("Q LV", "Q ductus")
set(gca,'FontSize',18.0)
title("Inflow 60% ductus & 40% AscAorta")

```

```

figure(6)
plot(time,Q_LV_7030,'LineWidth',3,'Color','r')
hold on;
plot(time,Q_ductus_7030,'LineWidth',3,'Color','b')
ylim([0 40]);
xlabel('Time (s)');
ylabel('Flow (ml/s)');
legend("Q LV", "Q ductus")
set(gca,'FontSize',18.0)
title("Inflow 70% ductus & 30% AscAorta")

```

```

figure(7)
plot(time,Q_LV_8020,'LineWidth',3,'Color','r')
hold on;
plot(time,Q_ductus_8020,'LineWidth',3,'Color','b')
ylim([0 40]);
xlabel('Time (s)');
ylabel('Flow (ml/s)');
legend("Q LV", "Q ductus")
set(gca,'FontSize',18.0)
title("Inflow 80% ductus & 20% AscAorta")

```

```

figure(8)
plot(time,Q_LV_9010,'LineWidth',3,'Color','r')
hold on;
plot(time,Q_ductus_9010,'LineWidth',3,'Color','b')
ylim([0 40]);
xlabel('Time (s)');
ylabel('Flow (ml/s)');
legend("Q LV", "Q ductus")
set(gca,'FontSize',18.0)
title("Inflow 90% ductus & 10% AscAorta")

```

## 12.2. CFD simulations with Sim Vascular

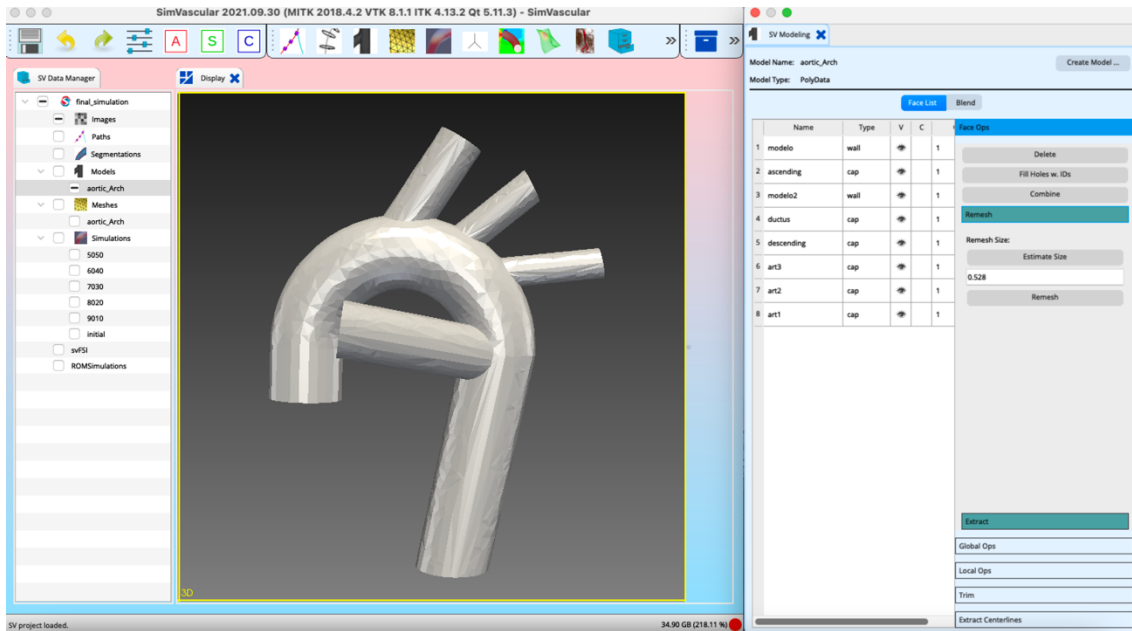


Figure 29. SV Modeling module in Sim Vascular with the imported solid model.

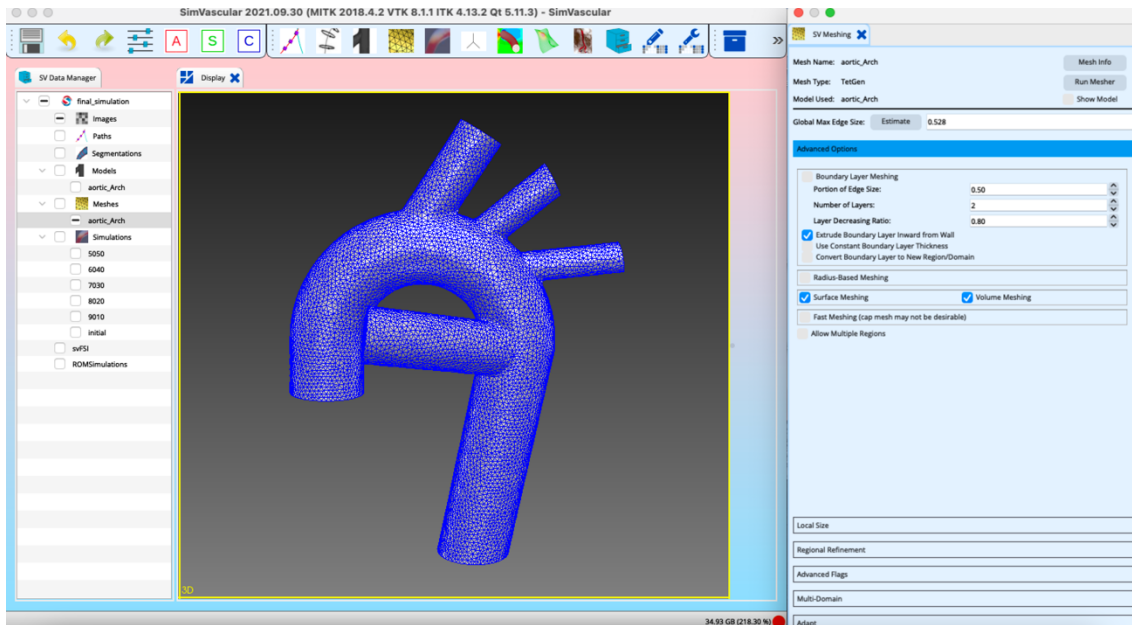
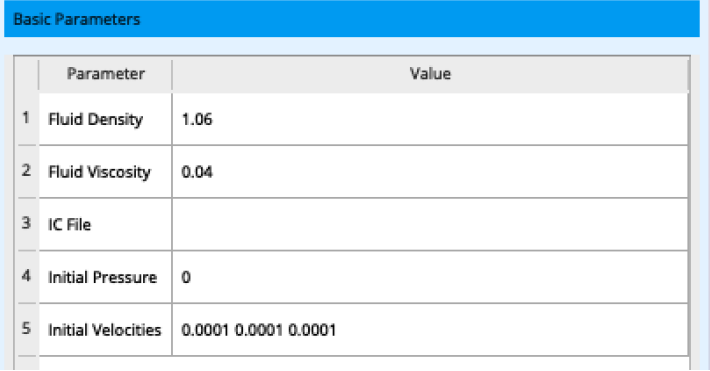
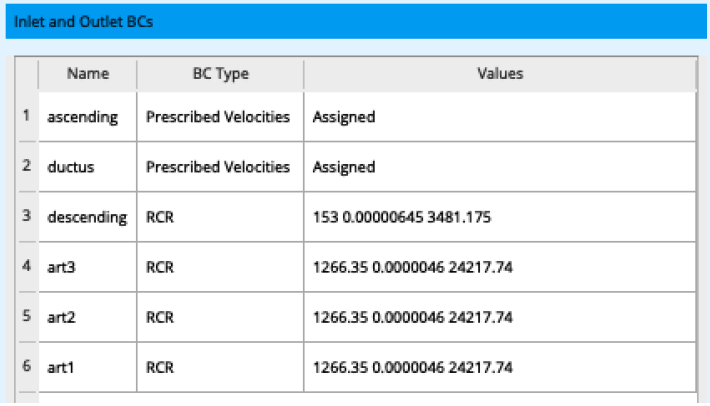
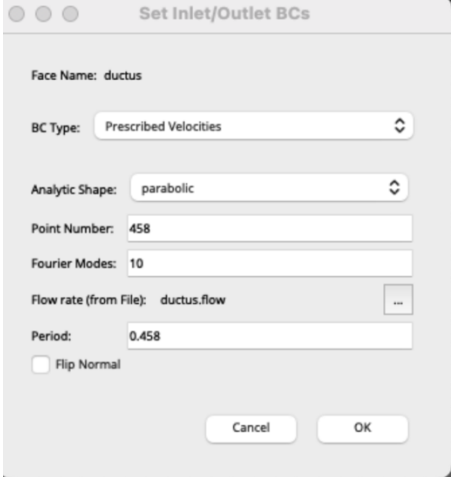
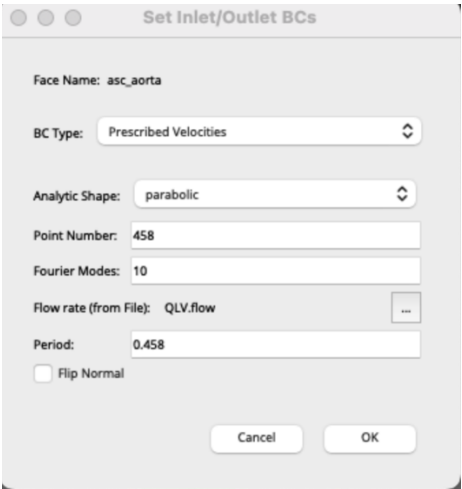
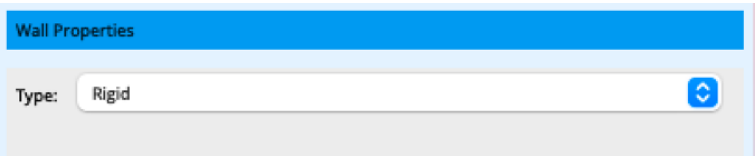
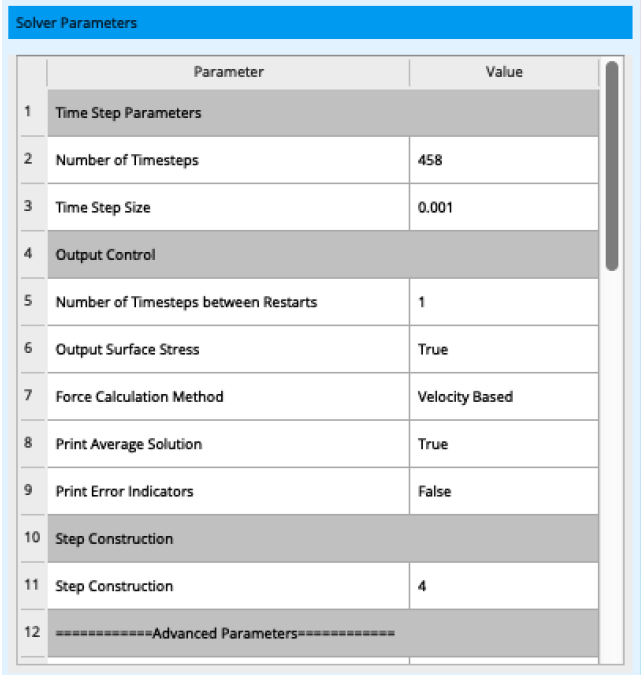


Figure 30. SV Meshing module in Sim Vascular with the generated 3D mesh.

## Sim Vascular Simulation Parameters

The table below contains the simulation steps which needed to be followed in order to run the CFD simulations in Sim Vascular.

<p><b>Basic parameters</b></p>	 <table border="1"> <thead> <tr> <th>Parameter</th> <th>Value</th> </tr> </thead> <tbody> <tr> <td>1 Fluid Density</td> <td>1.06</td> </tr> <tr> <td>2 Fluid Viscosity</td> <td>0.04</td> </tr> <tr> <td>3 IC File</td> <td></td> </tr> <tr> <td>4 Initial Pressure</td> <td>0</td> </tr> <tr> <td>5 Initial Velocities</td> <td>0.0001 0.0001 0.0001</td> </tr> </tbody> </table>		Parameter	Value	1 Fluid Density	1.06	2 Fluid Viscosity	0.04	3 IC File		4 Initial Pressure	0	5 Initial Velocities	0.0001 0.0001 0.0001									
Parameter	Value																						
1 Fluid Density	1.06																						
2 Fluid Viscosity	0.04																						
3 IC File																							
4 Initial Pressure	0																						
5 Initial Velocities	0.0001 0.0001 0.0001																						
<p><b>Inlet and Outlet Boundary Conditions Specification</b></p>	 <table border="1"> <thead> <tr> <th>Name</th> <th>BC Type</th> <th>Values</th> </tr> </thead> <tbody> <tr> <td>1 ascending</td> <td>Prescribed Velocities</td> <td>Assigned</td> </tr> <tr> <td>2 ductus</td> <td>Prescribed Velocities</td> <td>Assigned</td> </tr> <tr> <td>3 descending</td> <td>RCR</td> <td>153 0.00000645 3481.175</td> </tr> <tr> <td>4 art3</td> <td>RCR</td> <td>1266.35 0.0000046 24217.74</td> </tr> <tr> <td>5 art2</td> <td>RCR</td> <td>1266.35 0.0000046 24217.74</td> </tr> <tr> <td>6 art1</td> <td>RCR</td> <td>1266.35 0.0000046 24217.74</td> </tr> </tbody> </table>	Name	BC Type	Values	1 ascending	Prescribed Velocities	Assigned	2 ductus	Prescribed Velocities	Assigned	3 descending	RCR	153 0.00000645 3481.175	4 art3	RCR	1266.35 0.0000046 24217.74	5 art2	RCR	1266.35 0.0000046 24217.74	6 art1	RCR	1266.35 0.0000046 24217.74	<p><b>Inlet Boundary Conditions Specification – Cap Ductus</b></p> 
Name	BC Type	Values																					
1 ascending	Prescribed Velocities	Assigned																					
2 ductus	Prescribed Velocities	Assigned																					
3 descending	RCR	153 0.00000645 3481.175																					
4 art3	RCR	1266.35 0.0000046 24217.74																					
5 art2	RCR	1266.35 0.0000046 24217.74																					
6 art1	RCR	1266.35 0.0000046 24217.74																					

	<p><b>Inlet Boundary Conditions Specification – Cap Ascending Aorta</b></p>																																								
<p><b>Wall Properties Specification</b></p>																																									
<p><b>Solver Parameters</b></p>	 <table border="1" data-bbox="667 1234 1278 1839"> <thead> <tr> <th></th> <th>Parameter</th> <th>Value</th> </tr> </thead> <tbody> <tr> <td>1</td> <td colspan="2">Time Step Parameters</td> </tr> <tr> <td>2</td> <td>Number of Timesteps</td> <td>458</td> </tr> <tr> <td>3</td> <td>Time Step Size</td> <td>0.001</td> </tr> <tr> <td>4</td> <td colspan="2">Output Control</td> </tr> <tr> <td>5</td> <td>Number of Timesteps between Restarts</td> <td>1</td> </tr> <tr> <td>6</td> <td>Output Surface Stress</td> <td>True</td> </tr> <tr> <td>7</td> <td>Force Calculation Method</td> <td>Velocity Based</td> </tr> <tr> <td>8</td> <td>Print Average Solution</td> <td>True</td> </tr> <tr> <td>9</td> <td>Print Error Indicators</td> <td>False</td> </tr> <tr> <td>10</td> <td colspan="2">Step Construction</td> </tr> <tr> <td>11</td> <td>Step Construction</td> <td>4</td> </tr> <tr> <td>12</td> <td colspan="2">=====Advanced Parameters=====</td> </tr> </tbody> </table>			Parameter	Value	1	Time Step Parameters		2	Number of Timesteps	458	3	Time Step Size	0.001	4	Output Control		5	Number of Timesteps between Restarts	1	6	Output Surface Stress	True	7	Force Calculation Method	Velocity Based	8	Print Average Solution	True	9	Print Error Indicators	False	10	Step Construction		11	Step Construction	4	12	=====Advanced Parameters=====	
	Parameter	Value																																							
1	Time Step Parameters																																								
2	Number of Timesteps	458																																							
3	Time Step Size	0.001																																							
4	Output Control																																								
5	Number of Timesteps between Restarts	1																																							
6	Output Surface Stress	True																																							
7	Force Calculation Method	Velocity Based																																							
8	Print Average Solution	True																																							
9	Print Error Indicators	False																																							
10	Step Construction																																								
11	Step Construction	4																																							
12	=====Advanced Parameters=====																																								



### Solver Parameters

	Parameter	Value
12	-----Advanced Parameters-----	
13	Pressure Coupling	Implicit
14	Backflow Stabilization Coefficient	0.2
15	Non-linear Iteration Control	
16	Residual Control	True
17	Residual Criteria	0.001
18	Minimum Required Iterations	3
19	Linear Solver	
20	svLS Type	NS
21	Number of Krylov Vectors per GMRES Sweep	100
22	Number of Solves per Left-hand-side Formation	1
23	Tolerance on Momentum Equations	0.001

### Solver Parameters

	Parameter	Value
23	Tolerance on Momentum Equations	0.001
24	Tolerance on Continuity Equations	0.01
25	Tolerance on svLS NS Solver	0.01
26	Maximum Number of Iterations for svLS NS Solver	10
27	Maximum Number of Iterations for svLS Momentum Loop	10
28	Maximum Number of Iterations for svLS Continuity Loop	400
29	Discretization Control	
30	Time Integration Rule	Second Order
31	Time Integration Rho Infinity	0.5
32	Flow Advection Form	Convective
33	Quadrature Rule on Interior	2
34	Quadrature Rule on Boundary	3